Eur. Phys. J. C 27, 263–281 (2003)
Digital Object Identifier (DOI) 10.1140/epjc/s2002-01117-y

THE EUROPEAN PHYSICAL JOURNAL C

The reconstruction of supersymmetric theories at high energy scales

G.A. Blair[1,2], W. Porod[3], P.M. Zerwas[1]

[1] Deutsches Elektron-Synchrotron DESY, 22603 Hamburg, Germany
[2] Royal Holloway and Bedford New College, University of London, London, UK
[3] Institut für Theoretische Physik, Universität Zürich, 8057 Zürich, Switzerland

Received: 25 November 2002 /
Published online: 31 January 2003 –

Abstract. The reconstruction of fundamental parameters in supersymmetric theories requires the evolution to high scales, where the characteristic regularities in mechanisms of supersymmetry breaking become manifest. We have studied a set of representative examples in this context: minimal supergravity and a left–right symmetric extension; gauge mediated supersymmetry breaking; and superstring effective field theories. Through the evolution of the parameters from the electroweak scale the regularities in different scenarios at the high scales can be unravelled if precision analyses of the supersymmetric particle sector at e^+e^- linear colliders are combined with analyses at the LHC.

1 Introduction

Extending the standard model to a supersymmetric theory [1, 2] is an attractive step which has provided the qualitative understanding of a diverse set of phenomena in particle physics. Supersymmetry stabilizes the gap between the grand unification scale / Planck scale and the electroweak scale [3]. It allows the unification to be achieved of the three gauge couplings at a scale $M_U \simeq 2 \cdot 10^{16}$ GeV in a straightforward way [4]. Radiative electroweak symmetry breaking relates to the high value of the top mass [5]. Moreover, the cold dark-matter component in the universe can be identified with the lightest supersymmetric particle [6]. Above all, local supersymmetry, requiring the existence of massless spin 2 fields, provides a rationale for gravity [7].

Supersymmetry is not an exact symmetry in nature. Unraveling the breaking mechanism is therefore one of the central issues with this new concept. A variety of mechanisms have been proposed, based on rather different physical ideas. Among these schemes are supergravity theories [8] which have provided the framework for many phenomenological analyses. The suppression of flavor-changing neutral reactions is achieved in an automatic form within gauge mediated supersymmetry breaking [9]. Supersymmetry is broken in these scenarios in a hidden sector at high and intermediate scales, respectively, and the breaking is mediated by gravity or gauge interactions to the visible sector. The breaking, however, may not be communicated by direct action from the hidden to the visible sector. This is realized in anomaly mediated supersymmetry breaking models [10] in which supersymmetric particle masses are a consequence of the superconformal anomaly. In gaugino meditated supersymmetry breaking [11], supersymmetry is broken on a 3-brane separated from the 3-brane of the visible sector, and the breaking is communicated by gauge and Higgs superfields propagating through the 5-dimensional bulk. While in many models of supersymmetry breaking the gaugino masses are assumed to be universal at the unification scale, superstring motivated models, in which the breaking is moduli dominated, as opposed to dilaton dominated scenarios, give rise to non-universal boundary conditions at the high scale for the gauginos as well as the sfermion mass parameters [12, 13]. They can be exploited to determine the parameters of the string effective field theories.

In this report we elaborate on earlier investigations of [14] in which elements of gravity and gauge mediated supersymmetry breaking have been considered in realistic experimental environments of the proton collider LHC [15] and prospective TeV e^+e^- linear colliders [16, 17]. We extend these investigations in several directions in the present report.

In supergravity inspired models we adopt a scenario close to the Snowmass Point SPS#1 [18]. In a second step, the previous analysis, based on the minimal supersymmetric standard model, is extended to a left–right supersymmetric $SO(10)$ model [19]. The $SO(10)$ symmetry is assumed to be realized at a scale between the standard $SU(5)$ scale $M_U \simeq 2 \cdot 10^{16}$, derived from the unification of the gauge couplings, and the Planck scale $M_{\rm P} \simeq 10^{19}$ GeV. The right-handed neutrinos are assumed to be heavy, with masses at intermediate scales between $O(10^{10})$ GeV and $O(10^{15})$ GeV, so that the observed light neutrino masses are generated by the see-saw mechanism in a natural way [20]. A rough estimate of the intermediate scale follows

from the evolution of the mass parameters to the low experimental scale if universality holds at the grand unification scale.

In the gauge mediated symmetry breaking scenario, the fundamental scale is expected to be in the range from $O(10\,\mathrm{TeV})$ to $O(1\,\mathrm{EeV})$. We present an update and an extension of the earlier analysis. In particular, the effective supersymmetry breaking scales, the messenger and supersymmetric mass scales, can be reconstructed at the point where the masses of the sparticles carrying the same quantum numbers become identical, the characteristic regularity of gauge mediated supersymmetry breaking.

The anomaly mediated as well as the gaugino mediated SUSY breaking are technically equivalent to the mSUGRA case and will therefore not be treated explicitly again.

Among the most exciting schemes rank superstring induced scenarios (see e.g. [12, 13, 21] and references therein). In this report a string effective field theory, based on orbifold compactification of the heterotic string, will be analyzed at the phenomenological level. In the scenario considered, though dominated by the vacuum expectation values of the dilaton field, supersymmetry breaking is also affected by the moduli fields.

Such a mechanism gives rise to gaugino mass parameters with small but noticeable departure from universality, and non-universal sfermion mass parameters. From these mass parameters the fundamental parameters of the string effective field theory, such as the vacuum expectation values of the dilaton and the moduli fields, the moduli / dilaton mixing angle as well as the modular weights can be derived. In this way high-precision experiments can provide access to elements which are directly induced by superstrings [22].

Extrapolations over many orders of magnitude from the electroweak scale to scales near the Planck scale require high-precision measurements at the laboratory scale [23]. Such extrapolations can be performed in practice as demonstrated in the analysis of the electroweak and strong couplings at LEP and elsewhere [4]. The unification of these couplings provides the most compelling argument, derived from experiment, in support of supersymmetry. An initial set of precision data on supersymmetric particles is expected from LHC experiments if favorable cascade decays can be exploited to measure mass differences very precisely [15]. A globally comprehensive high-precision analysis can only be performed at lepton colliders [16, 17, 24–26]. They are expected to be realized in a first phase up to an energy of about 1 TeV, and in a subsequent second phase up to about 5 TeV. e^+e^- linear collider designs for the first phase are being worked out for JLC, NLC and TESLA, while the second phase may be realized in the CLIC technology. TESLA, in particular, can be operated at very high luminosity. A large number of threshold scans can therefore be performed which allows model independent high-precision measurements of the masses of supersymmetric particles. Chargino, neutralino and slepton masses are expected to be measured with accuracies at the per-mille level. Very heavy squarks and gluinos, on the other hand, may be analyzed in detail at CLIC after their discovery and first analysis at LHC. However, the accuracy is presumably reduced to the per-cent level as a consequence of the decreasing production cross sections, the non-zero widths of the heavy particles and the increasing energy smearing due to beam-strahlung.

Starting with observed numbers at the electroweak scale, the bottom–up approach exhausts all experimental information to the maximal extent possible in the empirical reconstruction of the underlying supersymmetric theory at the high scale. Finally, the parameters of the fundamental high-scale theory will become accessible in this way. This exploration of GUT and Planck scale physics by combining high precision with high energy in experiments at hadron and lepton colliders, is complemented by only a very small number of other methods, nota bene proton decay, likely neutrino physics, textures of mass matrices, and cosmology. In all these individual approaches only scarce information on the underlying physical structures at the GUT / Planck scale can be extracted. Any of these methods should therefore be exploited in the maximal form in order to shed light on the boundaries of the physics area where gravity may affect properties and interactions of particles observed in the laboratory at the electroweak scale. In this way consequences of incorporating the fourth of the fundamental forces into the particle system could become accessible at laboratory experiments.

2 Gravity mediated SUSY breaking

2.1 Minimal supergravity – mSUGRA

Supersymmetry cannot be broken spontaneously in our eigenworld without risking conflict with experimental results. The Ferrara–Girardello–Palumbo mass sum rule [27] requires supersymmetric particle masses below the corresponding standard model particle masses in this case – in obvious disagreement with observations. The elegant concept of spontaneous symmetry breaking, by non-perturbative gluino condensation for instance, can be realized, however, in a hidden sector which interacts with our eigenworld only by gravity. Gravitational interactions generate the soft supersymmetry breaking terms near the grand unification scale / Planck scale. Not compulsory but suggestive, the soft terms may be universal, i.e. the gaugino mass parameters and the scalar mass parameters[1]. Being flavor blind, the suppression of flavor-changing neutral processes can be realized in a natural way. Moreover, for a heavy top mass $m_t \simeq 174\,\mathrm{GeV}$ the breaking of the electroweak symmetry $SU(2)_\mathrm{L} \times U(1)_Y \to U(1)_\mathrm{EM}$ can be generated radiatively. While at the universality scale all scalar masses squared are positive, the Higgs mass parameter $M^2_{H_2}$ turns negative at a scale of about 10 PeV. This induces spontaneous electroweak symmetry breaking at the electroweak scale where the sum $M^2_{H_2}+|\mu|^2$ becomes

[1] Universality may be broken by GUT-scale threshold corrections, see e.g. [28]. The bottom–up approach should enable us to explore this domain in a systematic way to the maximum extent possible

negative, leaving however the strong and electromagnetic gauge symmetries $SU(3)_C$ and $U(1)_{\rm EM}$ unbroken.

The minimal supergravity scenario mSUGRA is characterized by the universal parameters of the gaugino mass parameter $M_{1/2}$, the scalar mass parameter M_0, and the trilinear coupling A_0, complemented by the phase of μ, the modulus $|\mu|$ determined by radiative symmetry breaking, and the mixing angle $\tan\beta$ in the Higgs sector.

The mass parameters $M_{1/2}$, M_0 and the trilinear coupling A_0 are defined to be universal at the grand unification scale M_U; the unified gauge coupling is denoted by α_U at M_U. For the sake of simplicity these parameters are taken real at the GUT scale. They are related to the low-energy parameters by the supersymmetric renormalization group equations [29, 30], which to leading order generate the evolution for

$$\text{the gauge couplings}: \alpha_i = Z_i \alpha_U, \tag{1}$$

$$\text{gaugino mass parameters}: M_i = Z_i M_{1/2}, \tag{2}$$

$$\text{scalar mass parameters}:$$

$$M^2_{\tilde{j}} = M_0^2 + c_j M_{1/2}^2 + \sum_{\beta=1}^{2} c'_{j\beta} \Delta M^2_\beta, \tag{3}$$

$$\text{trilinear couplings}: A_k = d_k A_0 + d'_k M_{1/2}. \tag{4}$$

The index i runs over the gauge groups $i = SU(3)$, $SU(2)$, $U(1)$. To leading order, the gauge couplings, and the gaugino and scalar mass parameters of soft supersymmetry breaking depend on the Z transporters

$$Z_i = \left[1 + b_i \frac{\alpha_U}{4\pi} \log\left(\frac{M_U}{M_Z}\right)^2\right]^{-1}, \tag{5}$$

with $b[SU_3, SU_2, U_1] = -3, 1, 33/5$; the scalar mass parameters depend also on the Yukawa couplings h_t, h_b, h_τ of the top quark, bottom quark and τ lepton.

The coefficients c_j [$j = L_l, E_l, Q_l, U_l, D_l, H_{1,2}$; $l = 1, 2, 3$] for the slepton and squark doublets / singlets of generation l, and for the two Higgs doublets are linear combinations of the evolution coefficients Z_i; the coefficients $c'_{j\beta}$ are of order unity. The shifts ΔM^2_β are nearly zero for the first two families of sfermions but they can be rather large for the third family and for the Higgs mass parameters, depending on the coefficients Z_i, the universal parameters M_0^2, $M_{1/2}$ and A_0, and on the Yukawa couplings h_t, h_b, h_τ. The coefficients d_k of the trilinear couplings A_k [$k = t, b, \tau$] depend on the corresponding Yukawa couplings and they are approximately unity for the first two generations while being $O(10^{-1})$ and smaller if the Yukawa couplings are large; the coefficients d'_k, depending on gauge and Yukawa couplings, are of order unity. Beyond the approximate solutions shown explicitly, the evolution equations have been solved numerically in the present analysis to two-loop order [30] and threshold effects have been incorporated at the low scale [31].

These parameters enter the mass matrices for the various particles. In the case of charginos $\tilde{\chi}^+_m$ [$m = 1, 2$] the 2×2 mass matrix reads

$$M_{\tilde{\chi}^+} = \begin{pmatrix} M_2 & \sqrt{2} m_W \cos\beta \\ \sqrt{2} m_W \sin\beta & \mu \end{pmatrix}, \tag{6}$$

while the mass matrix for the neutralinos $\tilde{\chi}^0_n$ [$n = 1, ..., 4$] is a 4×4 matrix,

$$M_{\tilde{\chi}^0} = \begin{pmatrix} M_1 & 0 & -m_Z c_\beta s_{\rm W} & m_Z s_\beta s_{\rm W} \\ 0 & M_2 & m_Z c_\beta c_{\rm W} & -m_Z s_\beta c_{\rm W} \\ -m_Z c_\beta s_{\rm W} & m_Z c_\beta c_{\rm W} & 0 & -\mu \\ m_Z s_\beta s_{\rm W} & -m_Z s_\beta c_{\rm W} & -\mu & 0 \end{pmatrix}. \tag{7}$$

Here, $s_\beta = \sin\beta$, $c_\beta = \cos\beta$ and $s_{\rm W}, c_{\rm W}$ are the sine and cosine of the electroweak mixing angle $\theta_{\rm W}$.

Exploiting all the information available from a linear collider, both mass matrices can be reconstructed even in the case of complex parameters [32]. For large values, $\tan\beta$ needs supplementary analyses in the Higgs sector [33].

Assuming that the sfermion generations mix only weakly, the mass matrices of the third generation sfermions can be written as

$$M^2_{\tilde{f}} = \begin{pmatrix} m^2_{\tilde{f}_{\rm L}} & m_f a_f \\ m_f a_f & m^2_{\tilde{f}_{\rm R}} \end{pmatrix}, \tag{8}$$

with

$$m^2_{\tilde{f}_{\rm L}} = M^2_{\tilde{F}_{\rm L}} + (T^3_f - e_f \sin^2\theta_{\rm W}) \cos 2\beta m_Z^2 + m_f^2, \tag{9}$$

$$m^2_{\tilde{f}_{\rm R}} = M^2_{\tilde{F}_{\rm R}} + e_f \sin^2\theta_{\rm W} \cos 2\beta m_Z^2 + m_f^2, \tag{10}$$

$$a_t \equiv A_t - \mu \cot\beta, a_b \equiv A_b - \mu \tan\beta,$$

$$a_\tau \equiv A_\tau - \mu \tan\beta, \tag{11}$$

where e_f and T^3_f are the electric charge and the third component of the weak isospin of the sfermion $\tilde{f}$; $M_{\tilde{F}_{\rm L}} = M_{\tilde{Q}}$ for $\tilde{f}_{\rm L} = \tilde{t}_{\rm L}, \tilde{b}_{\rm L}$, $M_{\tilde{F}} = M_{\tilde{L}}$ for $\tilde{f}_{\rm L} = \tilde{\tau}_{\rm L}, \tilde{\nu}_\tau$; $M_{\tilde{F}_{\rm R}} = M_{\tilde{U}}, M_{\tilde{D}}, M_{\tilde{E}}$ for $\tilde{f}_{\rm R} = \tilde{t}_{\rm R}, \tilde{b}_{\rm R}, \tilde{\tau}_{\rm R}$, respectively; m_f is the mass of the corresponding fermion. Also in this case it has been shown that the mass matrix can be reconstructed [34, 35]. The mass matrices for the first two generation sfermions have the same structure. However, due to the small fermion masses the mixing between the L/R sfermions can be neglected in general.

In the fits for the parameters we have used the complete one-loop mass matrices as given in [31]. For the Higgs bosons also the two-loop contributions [36] are included.

The mSUGRA point that we have analyzed in detail was chosen close to the Snowmass Point SPS#1 [18], except for the scalar mass parameter M_0 which was taken slightly larger for merely illustrative purpose: $M_{1/2} = 250\,{\rm GeV}$, $M_0 = 200\,{\rm GeV}$, $A_0 = -100\,{\rm GeV}$, $\tan\beta = 10$ and $\text{sign}(\mu) = +$. The initial "experimental" values have been generated by evolving the universal parameters down to the electroweak scale according to standard procedures [31, 37].

The parameters chosen are compatible with the present results of low-energy experiments which they affect by virtual contributions, and they are also compatible with dark-matter estimates [38]: $\text{BR}(b \to s\gamma) = 2.7 \cdot 10^{-4}$,

Table 1. Representative experimental mass errors used in the fits to the mass spectra; with the exception of the gluino mass, all the other parameters are based on LC measurements

Particle	M (GeV)	ΔM (GeV)	Particle	M (GeV)	ΔM (GeV)
h^0	113.33	0.05	$\tilde{\nu}_{e\mathrm{L}}$	256.79	0.11
H^0	436.1	1.5	$\tilde{e}_{\mathrm{L}}$	269.1	0.3
A^0	435.5	1.5	$\tilde{e}_{\mathrm{R}}$	224.82	0.15
$H^\pm$	443.3	1.5	$\tilde{\nu}_{\tau\mathrm{L}}$	255.63	0.95
$\tilde{\chi}_1^\pm$	183.05	0.15	$\tilde{\tau}_1$	217.7	1.0
$\tilde{\chi}_2^\pm$	383.3	0.3	$\tilde{\tau}_2$	271.5	0.9
$\tilde{\chi}_1^0$	97.9	0.2	$\tilde{u}_{\mathrm{L}}$	589	10
$\tilde{\chi}_2^0$	184.6	0.3	$\tilde{u}_{\mathrm{R}}$	572	10
$\tilde{\chi}_3^0$	365.5	0.3	$\tilde{d}_{\mathrm{R}}$	572	10
$\tilde{\chi}_4^0$	383.0	0.7	$\tilde{t}_1$	412	10
$\tilde{g}$	598	10	$\tilde{t}_2$	600	10

$\Delta[g-2]_\mu = 17 \cdot 10^{-10}$, $\Delta\rho = 38 \cdot 10^{-5}$ and $\Omega h^2 = 0.4$. We have used the formulas given in [39] for the computation of $b \to s\gamma$, those given in [40] for $\Delta[g-2]_\mu$, and those given in [41] for $\Delta\rho$; Ωh^2 has been calculated using the program of [42].

The five basic parameters define the experimental observables, including supersymmetric particle masses and production cross sections. They are endowed with errors as expected for threshold scans as well as measurements in the continuum at e^+e^- linear colliders (LC). Major parts of the LC analysis can be performed for energies below 1 TeV; some of the squarks require energies above 1 TeV. Estimates are based on integrated LC luminosities of $1\,\mathrm{ab}^{-1}$.

The errors given in [25] are scaled in proportion to the masses of the spectrum. Typical examples are shown in Table 1. The LC errors on the squark masses, see e.g. [43], are set to an average value of 10 GeV [similar errors may also be obtained if the precisely measured mass differences at the LHC are combined with high-precision measurements of the low-lying states at the LC]; varying this error within a factor two does not change the conclusions significantly since the measurement of the cross sections provides the maximal sensitivity in this sector. For the cross sections we use purely statistical errors, while assuming a (conservative) reconstruction efficiency of 20%. In addition the mass errors on the lightest gauginos were inflated with respect to earlier analyses to be conservative in advance of detailed experimental analyses of models with higher values of $\tan\beta$. [Parameter combinations from the fits to the spectrum and the cross sections which lead to charge and/or color breaking minima [44], are not accepted.]

These observables are interpreted as the experimental input values for the evolution of the mass parameters in the bottom–up approach to the grand unification scale.

2.1.1 Gauge couplings

The presumably strongest support, though indirect, for supersymmetry is related to the tremendous success of this theory in predicting the unification of the gauge couplings [4]. The precision, being at the per-cent level, is surprisingly high after extrapolations over fourteen orders of magnitude in the energy from the electroweak scale to the unification scale M_U. Conversely, the electroweak mixing angle has been predicted in this approach at the per-mille level. The evolution of the gauge couplings from low energy to the GUT scale M_U is carried out to two-loop accuracy. The gauge couplings g_1, g_2, g_3 and the Yukawa couplings are calculated in the $\overline{\mathrm{DR}}$ scheme by adopting the shifts given in [31]. These parameters are evolved to M_U using two-loop RGEs [30]. At two-loop order the gauge couplings do not meet exactly [45, 46], the differences owing to threshold effects at the unification scale M_U which leave us with an ambiguity in the definition of M_U. In this report we define M_U as the scale, ad libitum, where $g_1 = g_2$ in the RGE evolution. The non-zero difference $g_1 - g_3$ at this scale is then attributed to threshold effects of particles with masses of order M_U. The quantitative evolution implies important constraints on the particle content at M_U [47–51].

Table 2. Expected errors on M_U and α_U for the mSUGRA reference point, derived for the present level of accuracy and compared with GigaZ

	Now	GigaZ
M_U	$(2.00 \pm 0.06) \cdot 10^{16}$GeV	$(2.000 \pm 0.016) \cdot 10^{16}$GeV
α_U^{-1}	24.364 ± 0.015	24.361 ± 0.007

Based on the set of low-energy gauge and Yukawa parameters $\{\alpha(m_Z),\ \sin^2\theta_{\mathrm{W}},\ \alpha_{\mathrm{s}}(m_Z),\ Y_t(m_Z),\ Y_b(m_Z),\ Y_\tau(m_Z)\}$ the evolution of the inverse couplings α_i^{-1} [$i = U(1),\ SU(2),\ SU(3)$] is depicted in Fig. 1a. The evolution is performed for the mSUGRA reference point defined above. Unlike earlier analyses, the low-energy thresholds of supersymmetric particles can be calculated in this framework exactly without reference to effective SUSY scales. The broken error ellipse in Fig. 1b, derived for $[M_U, \alpha_U]$ by requiring $g_1 = g_2$, corresponds to the present experimental accuracy of the gauge couplings [52]: $\Delta\{\alpha^{-1}(m_Z),\ \sin^2\theta_{\mathrm{W}},\ \alpha_{\mathrm{s}}(m_Z)\} = \{0.03, 1.7 \cdot 10^{-4}, 3 \cdot 10^{-3}\}$. The full ellipse demonstrates the improvement for the absolute errors $\{10^{-3}, 10^{-5}, 10^{-3}\}$ after operating GigaZ [53, 54]. The expected accuracies in M_U and α_U are summarized in the values given in Table 2. The difference between the unification point in the ellipse and the value of g_3 is accounted for by contributions from high-scale physics, color-triplet Higgs fields, for example. Thus, for a typical set of SUSY parameters, the evolution of the gauge couplings from low to high scales leads to a precision of 1.5 per-cent of the grand unification picture.

2.1.2 Gaugino and scalar mass parameters

The results for the evolution of the mass parameters to the GUT scale M_U are shown in Fig. 2. Figure 2a presents the evolution of the gaugino parameters M_i^{-1} which clearly is under excellent control, as is the extrapolation of the

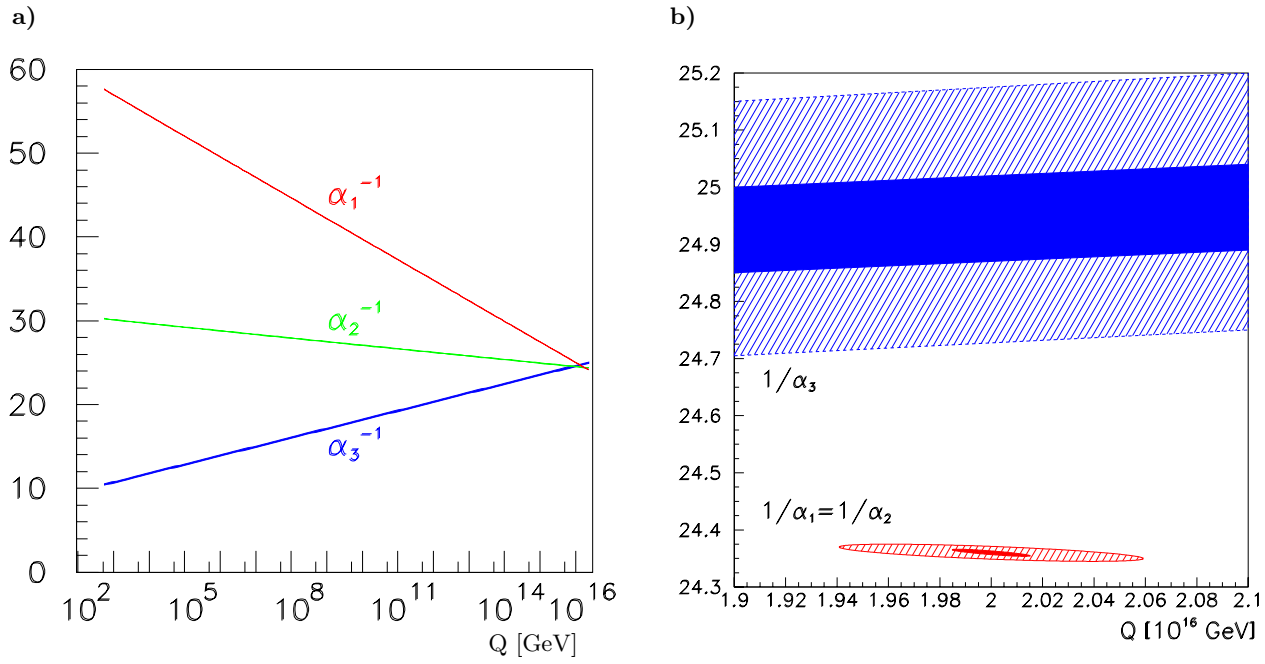

Fig. 1. a Running of the inverse gauge couplings. **b** Determination of M_U, α_U^{-1}; the unification point U is defined by the meeting point of α_1 with α_2. The wide error bands are based on present data; the narrow bands demonstrate the improvement expected by future GigaZ analyses

slepton mass parameter squared of the first (and second) and the third generation in Fig. 2c,d, respectively. The accuracy deteriorates for the squark mass parameters and for the Higgs mass parameter $M^2_{H_2}$. The origin of the differences between the errors for slepton, squark and Higgs mass parameters can be traced back to the numerical size of the coefficients in (3). Typical examples using the formulas presented in Appendix B evaluated at $Q = 500\,\mathrm{GeV}$ read as follows:

$$M^2_{\tilde{L}_1} \simeq M_0^2 + 0.47 M^2_{1/2}, \quad (12)$$

$$M^2_{\tilde{Q}_1} \simeq M_0^2 + 5.0 M^2_{1/2}, \quad (13)$$

$$M^2_{H_2} \simeq -0.03 M_0^2 - 1.34 M^2_{1/2} + 1.5 A_0 M_{1/2} + 0.6 A_0^2, \quad (14)$$

$$|\mu|^2 \simeq 0.03 M_0^2 + 1.17 M^2_{1/2} - 2.0 A_0 M_{1/2} - 0.9 A_0^2. \quad (15)$$

While the coefficients for sleptons are of order unity, the coefficient c_j for the squarks grows very large, $c_j \simeq 5.0$, so that small errors in $M^2_{1/2}$ are magnified by nearly an order of magnitude in the solution for M_0. By close inspection of (3) for the Higgs mass parameter it turns out that the formally leading M_0^2 part is nearly cancelled by the M_0^2 part of $c'_{j,\beta} \Delta M^2_\beta$. Inverting (3) for M_0^2 therefore gives rise to large errors in the Higgs case. A representative set of mass values and the associated errors, after evolution from the electroweak scale to M_U, is presented in Table 3. The corresponding error ellipses for the unification of the gaugino masses are shown in Fig. 2b.

Extracting the trilinear parameters A_k is difficult and more refined analyses based on sfermion cross sections and Higgs and/or sfermion decays are necessary to determine these parameters accurately.

Table 3. Representative gaugino / scalar mass parameters and couplings as determined at the electroweak scale and evolved to the GUT scale in the mSUGRA scenario; based on LHC and LC simulations. $M^2_{\tilde{L}_{1,3}}$, $M^2_{\tilde{Q}_{1,3}}$ are the slepton and squark isodoublet parameters of the first and third family whereas $M^2_{\tilde{E}_{1,3}}$, $M^2_{\tilde{U}_{1,3}}$ and $M^2_{\tilde{D}_{1,3}}$ are the slepton and squark isosinglet parameters of the first and third family. [The errors quoted correspond to 1σ.]

	Exp. input	GUT value
M_1 [GeV]	102.31 ± 0.25	250.00 ± 0.33
M_2 [GeV]	192.24 ± 0.48	250.00 ± 0.52
M_3 [GeV]	586 ± 12	250.0 ± 5.3
μ	358.23 ± 0.28	355.6 ± 1.2
$M^2_{\tilde{L}_1}$ [GeV^2]	$(6.768 \pm 0.005) \cdot 10^4$	$(3.99 \pm 0.41) \cdot 10^4$
$M^2_{\tilde{E}_1}$ [GeV^2]	$(4.835 \pm 0.007) \cdot 10^4$	$(4.02 \pm 0.82) \cdot 10^4$
$M^2_{\tilde{Q}_1}$ [GeV^2]	$(3.27 \pm 0.08) \cdot 10^5$	$(3.9 \pm 1.5) \cdot 10^4$
$M^2_{\tilde{U}_1}$ [GeV^2]	$(3.05 \pm 0.11) \cdot 10^5$	$(3.9 \pm 1.9) \cdot 10^4$
$M^2_{\tilde{D}_1}$ [GeV^2]	$(3.05 \pm 0.11) \cdot 10^5$	$(4.0 \pm 1.9) \cdot 10^4$
$M^2_{\tilde{L}_3}$ [GeV^2]	$(6.711 \pm 0.050) \cdot 10^4$	$(4.00 \pm 0.41) \cdot 10^4$
$M^2_{\tilde{E}_3}$ [GeV^2]	$(4.700 \pm 0.087) \cdot 10^4$	$(4.03 \pm 0.83) \cdot 10^4$
$M^2_{\tilde{Q}_3}$ [GeV^2]	$(2.65 \pm 0.10) \cdot 10^5$	$(4.1 \pm 3.0) \cdot 10^4$
$M^2_{\tilde{U}_3}$ [GeV^2]	$(1.86 \pm 0.12) \cdot 10^5$	$(4.0 \pm 3.6) \cdot 10^4$
$M^2_{\tilde{D}_3}$ [GeV^2]	$(3.03 \pm 0.12) \cdot 10^5$	$(4.0 \pm 2.6) \cdot 10^4$
$M^2_{H_1}$ [GeV^2]	$(6.21 \pm 0.08) \cdot 10^4$	$(4.01 \pm 0.54) \cdot 10^4$
$M^2_{H_2}$ [GeV^2]	$(-1.298 \pm 0.004) \cdot 10^5$	$(4.1 \pm 3.2) \cdot 10^4$
A_t [GeV]	-446 ± 14	-100 ± 54
$\tan\beta$	9.9 ± 0.9	–

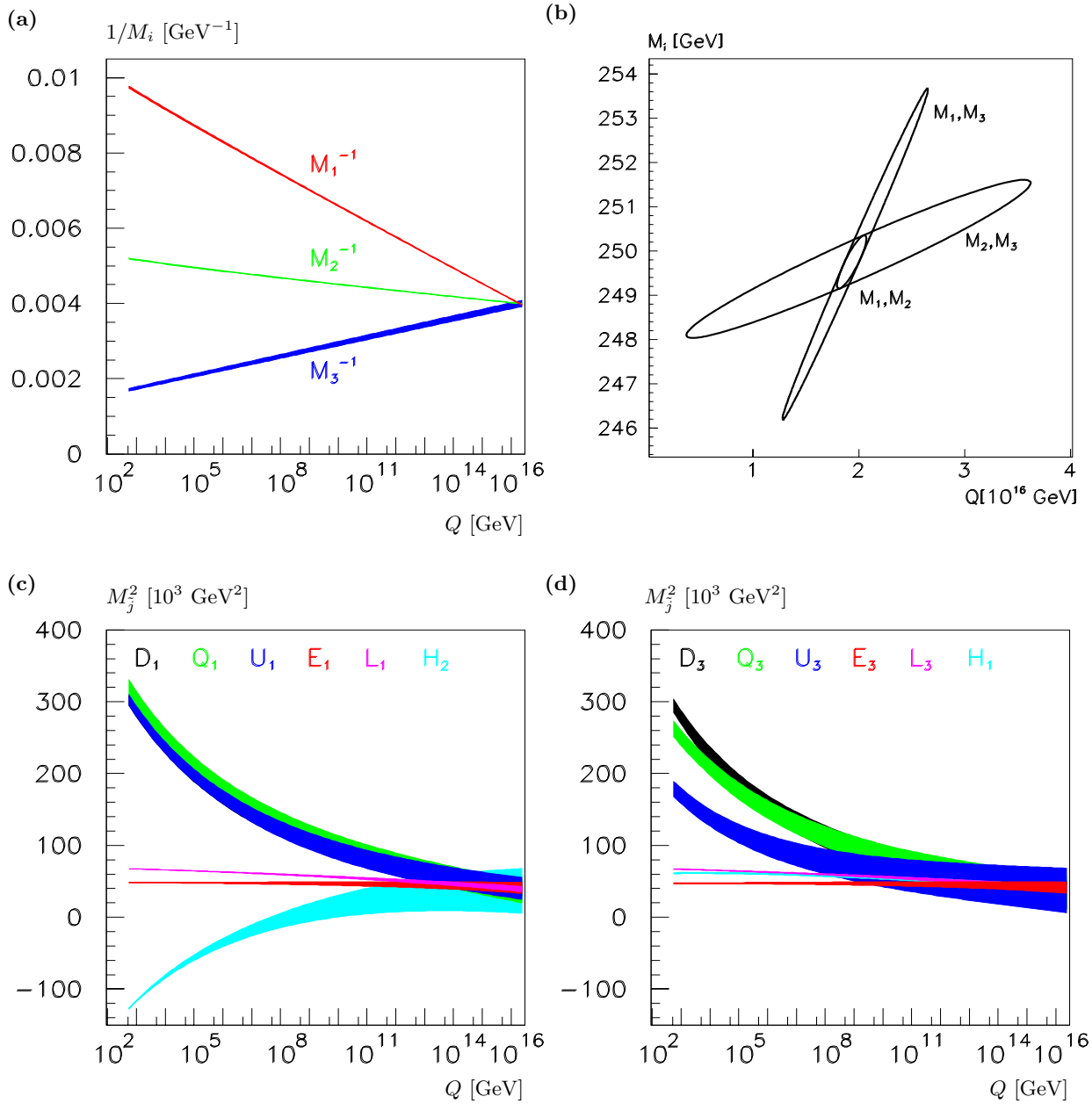

Fig. 2a–d. mSUGRA: Evolution, from low to high scales, of **a** gaugino mass parameters, and **b** unification of gaugino mass parameter pairs; **c** evolution of first-generation sfermion mass parameters and the Higgs mass parameter $M_{H_2}^2$; **d** evolution of third-generation sfermion mass parameters and the Higgs mass parameter $M_{H_1}^2$. The mSUGRA point probed is defined by the parameters $M_0 = 200\,\text{GeV}$, $M_{1/2} = 250\,\text{GeV}$, $A_0 = \text{-}100\,\text{GeV}$, $\tan\beta = 10$, and $\text{sign}(\mu) = (+)$. [The widths of the bands indicate the 1σ CL.]

A_t can be obtained from the mixing angle of the stop sector by measuring the stop production cross section in e^+e^- annihilation with different electron and/or positron polarizations [35]. In the cases A_b and A_τ the situation is more difficult, because these parameters influence the mixing angle in the sbottom and stau sector only weakly as is evident from (11). In these cases the $\tilde{b}$ and $\tilde{\tau}$ couplings to the Higgs bosons must be measured, because these couplings include terms directly proportional to $A_k \tan\beta$. For instance, by analyzing the decays $\tilde{\tau}_2 \to A^0\tilde{\tau}_1$, $h^0\tilde{\tau}_1$ and $H^0\tilde{\tau}_1$, A_τ can be extracted within 10% [34]. If these modes are kinematically forbidden, the couplings can either be measured in the decays of the heavier Higgs bosons, as $H^0, A^0 \to \tilde{\tau}_1\tilde{\tau}_1$, or by means of the cross sections for processes such as $e^+e^- \to \tilde{\tau}_1\tilde{\tau}_1 h^0$. Similar procedures are expected to apply for A_b. In certain areas of the SUSY parameter space, the trilinear couplings can also be extracted from measurements of the degree of the fermion polarization [55] in sfermion decays $\tilde{t}, \tilde{b}$ and $\tilde{\tau}$.

The unified value A_0 of the A_t coupling, the best measured coupling among the A_k parameters, is shielded by the pseudo-fixed point behavior of A_t [56] since $d_t \simeq 0.2$

Table 4. Comparison of the ideal parameters with the experimental expectations for the particular mSUGRA reference point analyzed in this report. [All mass parameters are given in units of GeV.]

	Ideal	Experimental error
M_U	$2 \cdot 10^{16}$	$1.6 \cdot 10^{14}$
α_U^{-1}	24.361	0.007
$M_{1/2}$	250	0.08
M_0	200	0.09
A_0	-100	1.8
μ	358.23	0.21
$\tan\beta$	10	0.1

is small compared to $d_t' \simeq 2$. The impact of the other trilinear couplings on physical observables is weak so that large experimental errors are expected. As a result, the universal character of the fundamental parameter A_0 cannot be determined as precisely as the other parameters at the GUT scale.

Although the trilinear couplings A_b and A_τ have only little impact on the physical observables, they do strongly influence the running of the third-generation sfermion mass parameters as well as the Higgs mass parameters. The error propagation is stabilized if A_τ and A_b can be measured in the way outlined above. [Otherwise the errors would increase by an order of magnitude.] The detailed analysis in this report has been based on the auxiliary assumption that A_b and A_τ are within 1σ of $A_t = A_0$ at M_U; this assumption is conservative if the envisaged experimental analyses of A_τ and A_b can be performed at the electroweak scale indeed.

Even though the auxiliary assumption seems conservative, given the size of the error on A_0 determined from A_t, dedicated phenomenological and experimental analyses of the third family must be developed, as indicated above, to improve the measurement of the associated parameters, in particular in view of the evolution of the Higgs mass parameter which induces electroweak symmetry breaking.

Inspecting Fig. 2c,d leads to the conclusion that a blind top–down approach eventually generates an incomplete picture. Global fits based on mSUGRA without allowing for deviations from universality are dominated by $M_{1,2}$ and the slepton mass parameters due to the pseudo-fixed point behavior of the squark mass parameters. Therefore, the structure of the theory in the squark sector is not scrutinized stringently at the unification scale in the top–down approach, let alone the Higgs sector. By contrast, the bottom–up approach demonstrates very clearly the extent to which the theory can be tested at the high scale quantitatively.

The quality of the test is apparent from Table 3, in which the evolved gaugino values should reproduce the universal mass $M_{1/2} = 250\,\text{GeV}$ and all the scalars the mass $M_0 = 200\,\text{GeV}$. They are compared with the global mSUGRA fit of the universal parameters in Table 4.

2.2 Left–right supergravity

It is generally accepted that neutrinos are massive particles, though at a very low scale. Supersymmetric scenarios like MSSM and mSUGRA must therefore be extended to incorporate the right-handed neutrino degrees of freedom. Since the complexity grows strongly with the increasing number of parameters, it is useful, in a first attempt, to analyze the system in characteristic scenarios based on compelling physical assumptions. In particular, we will assume that the small neutrino masses are generated by the seesaw mechanism [20]. Moreover, we will assume hierarchies for the heavy neutrino masses as well as the neutrino Yukawa couplings similar to the up-type particles in the quark sector; such a scheme, suggested by $SO(10)$ GUT, is compatible with the data collected in low-energy neutrino experiments [57].

This scenario can be embedded in a grand unified $SO(10)$ theory with the following breaking pattern of the symmetries. The $SO(10)$ symmetry is realized between the Planck scale M_P and a scale $M_{SO(10)}$ at which the symmetry breaks to $SU(5)$. The scale $M_{SO(10)}$ is assumed above the scale M_U where $SU(5)$ breaks to the symmetry group $SU(3)_C \times SU(2)_\text{L} \times U(1)_Y$ of the standard model. At the scale M_U the gauge couplings split and the effective theory is the MSSM plus right-handed neutrinos with masses of order 10^9 to $10^{15}\,\text{GeV}$. Below this mass scale the right-handed neutrinos freeze out and the MSSM is effectively realized in its standard form. The relevant SUSY parameters are summarized in Table 5. It is less obvious that M_U associated with the $SU(5)$ symmetry is the scale where the gaugino and scalar mass parameters are universal. The supporting argument for this point is derived empirically from the unification of the gauge couplings. Nevertheless, the subsequent analysis will be based on this hypothesis which, of course, is a clear target for confirmation or rejection in the bottom–up approach we investigate[2].

In this left–right supergravity point, called LR-SUGRA for short[3], we have probed the same SUSY parameters as above, complemented by the same universal parameters in the right-handed sneutrino sector. The sneutrinos $\tilde{\nu}_\text{L}$ and $\tilde{\nu}_\text{R}$ mix by the (large) Yukawa interactions in the $\hat{\nu}_\text{R}$ sector of the superpotential to form the mass eigenstates $\tilde{\nu}_1$ and $\tilde{\nu}_2$. Also in this sector an effective seesaw mechanism is induced by the large ν_R mass, as can be most easily seen by considering the one-generation case:

$$m^2 = \begin{pmatrix} M_{\tilde{L}}^2 + \frac{1}{2} m_Z^2 \cos 2\beta & \frac{1}{\sqrt{2}} Y_\nu (A_\nu v_2 - \mu v_1) \\ \frac{1}{\sqrt{2}} Y_\nu (A_\nu v_2 - \mu v_1) & M_{\tilde{N}}^2 + M_{\nu_\text{R}}^2 \end{pmatrix}. \quad (16)$$

[2] Potential sources of deviations from this picture can easily be illustrated by assuming $M_{SO(10)}$ as the scale proper of universality: The Yukawa interactions contribute differently to the running of the $M_{\bar{10}}^2$, $M_{\bar{5}}^2$, $M_{\tilde{N}}^2$; the same holds true for the A parameters [58]. Moreover, different D-term contributions to the scalar masses are in general generated by the breaking mechanism from $SO(10)$ to $SU(5)$ [59]

[3] Other left–right scenarios will be presented in a forthcoming publication

Table 5. Scales and soft SUSY breaking parameters of the effective left–right supergravity theory LR-SUGRA analyzed in this report

Scale	Gauge group	Parameters
$M_{\rm P}$–$M_{SO(10)}$	$SO(10)$	$M_{1/2}$, $M^2_{\underline{16}}$, A_0
$M_{SO(10)}$–M_U	$SU(5)$	$M_{1/2}$, $M^2_{\underline{10}}$, $M^2_{\bar{5}}$
		$M^2_{\tilde{N}}$, A_{10}, A_5, A_ν
M_U–$M_{\nu_{\rm R}}$	$SU(3)_C \otimes SU(2)_{\rm L} \otimes U(1)_Y$	M_1, M_2, M_3
		$M^2_{\tilde{Q}}$, $M^2_{\tilde{U}}$, $M^2_{\tilde{D}}$
		$M^2_{\tilde{L}}$, $M^2_{\tilde{N}}$, $M^2_{\tilde{E}}$
		A_u, A_d, A_τ, A_ν
$M_{\nu_{\rm R}}$–$M_{\rm EW}$	$SU(3)_C \otimes SU(2)_{\rm L} \otimes U(1)_Y$	M_1, M_2, M_3
		$M^2_{\tilde{Q}}$, $M^2_{\tilde{U}}$, $M^2_{\tilde{D}}$
		$M^2_{\tilde{L}}$, $M^2_{\tilde{E}}$
		A_u, A_d, A_τ

In this mass matrix $M_{\nu_{\rm R}}$ is the [GUT-scale] mass of the right-handed neutrino, $M_{\tilde{N}}$ the scalar [TeV-scale] mass parameter of the right sneutrino, Y_ν and A_ν the neutrino Yukawa coupling and the neutrino trilinear coupling, respectively. v_1 and v_2 are the vacuum expectation values of the Higgs field with isospin $-1/2$ and isospin $1/2$, respectively. The approximate eigenvalues of the sneutrino mass matrix read

$$m^2_{\tilde{\nu}_1} \simeq M^2_{\tilde{L}} + \frac{1}{2} m^2_Z \cos 2\beta - Y^2_\nu \frac{(A_\nu v_2 - \mu v_1)^2}{2M^2_{\nu_{\rm R}}}, \quad (17)$$

$$m^2_{\tilde{\nu}_2} \simeq M^2_{\nu_{\rm R}} + M^2_{\tilde{N}} + Y^2_\nu \frac{(A_\nu v_2 - \mu v_1)^2}{2M^2_{\nu_{\rm R}}}. \quad (18)$$

The $\tilde{\nu}_{\rm R}$ mass is close to the large GUT-scale $\nu_{\rm R}$ mass and not to the TeV-scale mass parameter $M_{\tilde{N}}$ – as anticipated by the Yukawa term in the diagonal RR matrix element of (16). The rotation of the current to the mass eigenstates

$$\tilde{\nu}_1 = \cos\theta_{\tilde{\nu}} \tilde{\nu}_{\rm L} + \sin\theta_{\tilde{\nu}} \tilde{\nu}_{\rm R}, \quad (19)$$

$$\tilde{\nu}_2 = -\sin\theta_{\tilde{\nu}} \tilde{\nu}_{\rm L} + \cos\theta_{\tilde{\nu}} \tilde{\nu}_{\rm R} \quad (20)$$

is described by a small mixing angle,

$$\sin\theta_{\tilde{\nu}} \simeq Y_\nu |A_\nu v_2 - \mu v_1| / (\sqrt{2} M^2_{\nu_{\rm R}}), \quad (21)$$

$$\cos\theta_{\tilde{\nu}} \simeq 1. \quad (22)$$

Thus, to a very good approximation, $\tilde{\nu}_1$ coincides with $\tilde{\nu}_{\rm L}$, and $\tilde{\nu}_2$ with $\tilde{\nu}_{\rm R}$.

The heavy right-handed neutrino masses are calculated by identifying the Yukawa couplings with the up-type quark couplings in the quark sector at the GUT scale (largely equivalent to the $SO(10)$ scale in this regard) and by identifying the light neutrino masses with the neutrino mass differences in the large mixing angle for the solar neutrino problem solution: $m_{\nu_{\rm L_1}} = 10^{-5}\,$eV, $m_{\nu_{\rm L_2}} = 3{\cdot}10^{-3}\,$eV, $m_{\nu_{\rm L_3}} = 6{\cdot}10^{-2}\,$eV; $M_{\nu_{\rm R_1}} = 3{\cdot}10^9\,$GeV, $M_{\nu_{\rm R_2}} = 1.4 \cdot 10^{11}\,$GeV, $M_{\nu_{\rm R_3}} = 1.7 \cdot 10^{14}\,$GeV.

The impact on the evolution of the mass parameters is rather simple. In the analysis of the first two generations the Yukawa interactions involving the heavy neutrinos and the R-sneutrinos are so small that their effect is not noticeable in practice. The evolution of the gaugino and scalar mass parameters is not affected by the left–right extension of the system in the present form as is evident from Fig. 3a,c. This is only different for the third generation and for $M^2_{H_2}$ owing to the enhanced Yukawa coupling in this case as shown in Figs. 3b,d. The sensitivity to the intermediate $\nu_{\rm R}$ scales remains rather weak however, because neutrino Yukawa couplings affect the evolution of the sfermion mass parameters only mildly.

Since the $\nu_{\rm R}$ of the third generation is unfrozen only beyond the scale $Q = M_{\nu_{\rm R}}$ the impact of the LR extension becomes visible in the evolution only at very high scales. In Fig. 3b we display the evolution of $M^2_{\tilde{E}_3}$, $M^2_{\tilde{L}_3}$ and $M^2_{H_2}$ for illustrative purposes. The full lines include the effects of the right-handed neutrino, which are to be compared with the dashed lines where the $\nu_{\rm R}$ sector is cut-off. The scalar mass parameter $M^2_{\tilde{E}_3}$ appears unaffected by the right-handed sector, while $M^2_{\tilde{L}_3}$ and $M^2_{H_2}$ clearly are. Only the picture including $\nu_{\rm R}$, $\tilde{\nu}_{\rm R}$ is compatible with the unification assumption. The kinks in the evolution of $M^2_{\tilde{L}_3}$ and $M^2_{H_2}$ can be traced back to the fact that around $10^{14}\,$GeV the third-generation (s)neutrinos become quantum mechanically effective, given a large enough neutrino Yukawa coupling to influence the evolution of these mass parameters.

A much better understanding of the third-generation family must be achieved to draw quantitative conclusions beyond the rough estimates of the $\nu_{\rm R}$ scales sketched in the present analysis.

3 Gauge mediated supersymmetry breaking

Motivated by the observed suppression of flavor-changing neutral transitions, supersymmetry breaking mediated by gauge interactions from a secluded sector to the visible eigenworld, offers an automatic solution to this problem [9, 60]. The scalar and the F components of a standard-model singlet superfield S acquire vacuum expectation values $\langle S \rangle$ and $\langle F_S \rangle$ through interactions with fields in the secluded sector, thus breaking supersymmetry[4].

Vector-like messenger fields M, carrying non-zero $SU(3) \times SU(2) \times U(1)$ charges and coupling to S, transport the supersymmetry breaking to the eigenworld.

The system is characterized by the mass $M_{\rm M} \sim \langle S \rangle$ of the messenger fields and the mass scale $\Lambda = \langle F_S \rangle / \langle S \rangle$ setting the size of the gaugino and scalar masses. $M_{\rm M}$ is expected to be in the range of 10 TeV to 1 EeV and Λ has

[4] A solution of the doublet-triplet splitting problem can be found in GMSB by introducing two different S fields. The masses of supersymmetric particles are less constrained in this approach than in the one-scale model, and they depend on the values of the two Λ_i parameters. In particular, the approximate equality of the gaugino masses at the GUT scale is lifted; see [61] for details

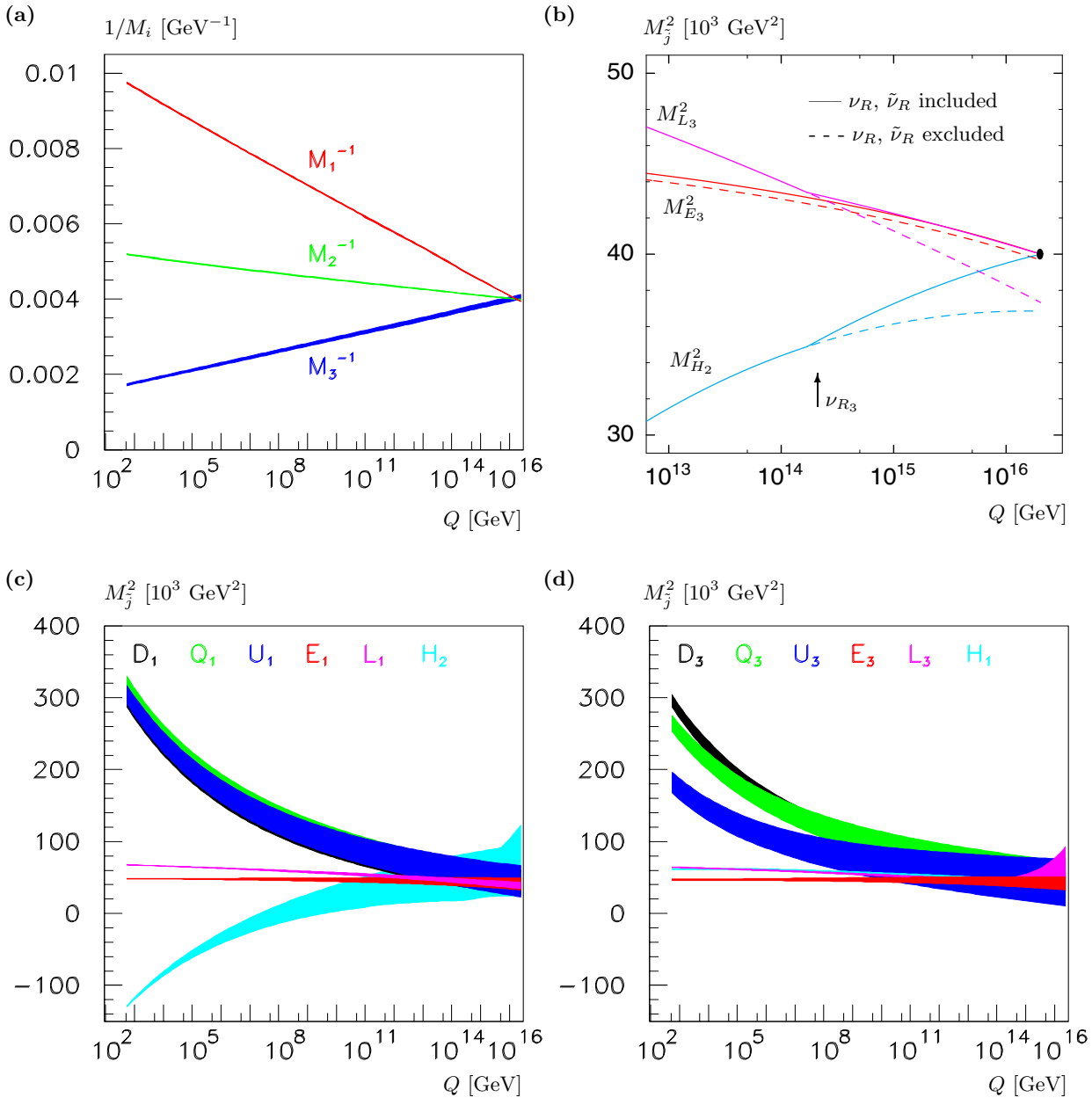

Fig. 3a–d. LR-SUGRA with $\nu_{\rm R}$: Evolution of **a** gaugino mass parameters; **b** evolution of third-generation slepton mass parameters and Higgs mass parameters $M_{H_2}^2$, with/out neutrino-R sector; **c** evolution of first-generation sfermion mass parameters and Higgs mass parameters $M_{H_2}^2$; **d** evolution of third-generation sfermion mass parameters and Higgs mass parameters $M_{H_1}^2$. The mSUGRA point probed is characterized by the parameters $M_0 = 200\,\text{GeV}$, $M_{1/2} = 250\,\text{GeV}$, $A_0 = -100\,\text{GeV}$, $\tan\beta = 10$, and $\text{sign}(\mu) = (+)$, while the $\nu_{\rm R3}$ scale is taken close to 10^{14} GeV. [The widths of the bands indicate the 1σ CL.]

to be smaller than $M_{\rm M}$. The gaugino masses

$$M_i(M_{\rm M}) = (N_5 + 3N_{10}) g\,(\Lambda/M_{\rm M})\,\alpha_i(M_{\rm M})\Lambda \qquad (23)$$

are generated by loops of the scalar and fermionic messenger component fields; N_i is the multiplicity of messengers in the $5 + \bar{5}$ and $10 + \overline{10}$ vector-like multiplets, and

$$g(x) = \frac{1+x}{x^2}\log(1+x) + (x \to -x) \qquad (24)$$

is the messenger-scale threshold function [62] which approaches unity for $\Lambda \ll M_{\rm M}$. Masses of the scalar fields in the visible sector are generated by two-loop effects of gauge / gaugino and messenger fields:

$$M_{\tilde{j}}^2(M_{\rm M}) = 2(N_5 + 3N_{10}) f\,(\Lambda/M_{\rm M}) \sum_{i=1}^{3} k_i C_j^i \alpha_i^2(M_{\rm M})\Lambda^2, \qquad (25)$$

with $k_i = 1, 1, 3/5$ for $SU(3)$, $SU(2)$, and $U(1)$, respectively; the coefficients C_j^i are the quadratic Casimir invariants, being 4/3, 3/4, and $Y^2/4$ for the fundamental representations $\tilde{j}$ in the groups $i = SU(3), SU(2)$ and $U(1)$,

with $Y = 2(Q - I_3)$ denoting the usual hypercharge; also the threshold function [62]

$$f(x) = \frac{1+x}{x^2}\left[\log(1+x) - 2\mathrm{Li}_2\left(\frac{x}{1+x}\right) + \frac{1}{2}\mathrm{Li}_2\left(\frac{2x}{1+x}\right)\right] + (x \to -x) \quad (26)$$

approaches unity for $\Lambda \ll M_{\mathrm{M}}$. As evident from (25), scalar particles with identical standard-model charges squared have equal masses at the messenger scale M_{M}.

In the minimal version of GMSB, the A parameters are generated at three-loop level and they are practically zero at M_{M}.

We have investigated this scheme for the point $\Lambda = 100\,\mathrm{TeV}$, $M_{\mathrm{M}} = 200\,\mathrm{TeV}$, $N_5 = 1$, $N_{10} = 0$, $\tan\beta = 15$ and $\mu > 0$ corresponding to the Snowmass Point SPS#8.

We find for the low-energy data: $\mathrm{BR}(b \to s\gamma) = 3.7 \cdot 10^{-4}$, $\Delta[g-2]_\mu = 15 \cdot 10^{-10}$, $\Delta\rho = 64 \cdot 10^{-5}$.

The evolution[5] of the gaugino and sfermion mass parameters of the first and third generation as well as the Higgs mass parameters, including two-loop β-functions, are presented in Fig. 4.

Owing to the influence of the A parameters in the two-loop RGEs for the gaugino mass parameters, the gaugino mass parameters do not meet at the same point as the gauge couplings in this scheme.

It is obvious from the figure that the GMSB scenario cannot be confused with the universal supergravity scenario[6]. [Specific experimental signatures generated in the decays of the next to lightest supersymmetric particle, the neutralino $\tilde{\chi}_1^0$ or the stau $\tilde{\tau}_1$, to gravitinos which are very light in GMSB, provide a complementary experimental discriminant; see [17, 64]].

The bands of the slepton L-doublet mass parameter $M_{\tilde{L}}^2$ and the Higgs parameter $M_{H_2}^2$, which carry the same moduli of standard-model charges, cross at the scale M_{M}. The crossing, which is indicated by an arrow in Fig. 4c, is a necessary condition (in the minimal form) for the GMSB scenario to be realized.

The two scales Λ and M_{M} can be extracted from the spectrum of the gaugino and scalar particles. Combining the two species allows one to determine the multiplicity coefficient $(N_5 + 3N_{10})$ in addition. The dependence of the spectra on Λ is, trivially, very strong. The messenger scale M_{M} can be determined only from the running of the masses between the messenger scale and the electroweak scale; despite being governed by weakly varying logarithms, the accuracy in determining M_{M} is surprisingly good. For the point analyzed in the example above, the following accuracy for the mass parameters and the messenger multiplicity has been found:

$$\Lambda = (1.01 \pm 0.03) \cdot 10^2\,\mathrm{TeV}, \quad (27)$$

[5] The same formulae as in Appendix B.1 apply for the GMSB boundary conditions at the electroweak scale by replacing M_U by M_{M}, the GMSB scale

[6] A comparison of the mass characteristics at the low scale between mSUGRA and GMSB in a top–down approach is presented in [63]

Table 6. Average ratios of the scalar mass parameters as predicted in GMSB solely by group factors and gauge couplings; compared at the 95% CL with the mSUGRA reference point

Mass^2 ratios	⟨GMSB⟩	≠mSUGRA
H_2^2/L_1^2	1	–
E_1^2/L_1^2	0.25	≥0.8
Q_1^2/L_1^2	8.87	≤3.2
U_1^2/L_1^2	8.03	≤ 3.0
D_1^2/L_1^2	7.95	≤3.2
H_1^2/L_1^2	1	≤1.0

$$M_{\mathrm{M}} = (1.92 \pm 0.24) \cdot 10^2\,\mathrm{TeV}, \quad (28)$$

$$N_5 + 3N_{10} = 0.978 \pm 0.056. \quad (29)$$

The correlation between Λ and M_{M} is shown in Fig. 4b.

While the gaugino masses in GMSB evolve nearly in the same way as in mSUGRA, the running of the scalar masses is quite different in both theories. Moreover, at the messenger scale the ratios of scalar masses squared in the simplest version of GMSB are determined solely by group factors and gauge couplings, being independent of the specific GMSB characteristics, i.e. messenger multiplicities and Λ mass scale:

$$\frac{M_j^2(M_{\mathrm{M}})}{M_{j'}^2(M_{\mathrm{M}})} = \frac{\sum_{i=1}^3 k_i C_i^j \alpha_i^2(M_{\mathrm{M}})}{\sum_{i=1}^3 k_i C_i^{j'} \alpha_i^2(M_{\mathrm{M}})}. \quad (30)$$

The predictions for these ratios are listed in Table 6. The ratios in GMSB are distinctly different from the ratios in mSUGRA, taken at the scale where the upper boundary of the 2σ band for H_2^2/L_1^2 approaches unity from below. [Ideally all ratios approach unity only at the grand unification scale M_U in mSUGRA.] The distinct differences between GMSB and mSUGRA are clearly visible in Figs. 5a versus b.

4 String induced supersymmetry breaking

In the previously analyzed SUGRA and GMSB models the structure of the supersymmetry breaking mechanisms *sui generis* and the fields involved in the hidden sectors are shielded from the eigenworld. Four-dimensional strings naturally give rise to a minimal set of fields for inducing supersymmetry breaking; they play the rôle of the fields in the hidden sectors: the dilaton S and the moduli T_m chiral superfields which are generically present in large classes of 4-dimensional heterotic string theories[7]. The vacuum expectation values of S and T_m, generated by genuinely non-perturbative effects, determine the soft supersymmetry breaking parameters. In this approach, which we will adopt for a characteristic case study without reference to open theoretical problems of dilaton / moduli field stabilization, grand unification at the standard scale can be

[7] For other scenarios see [65]

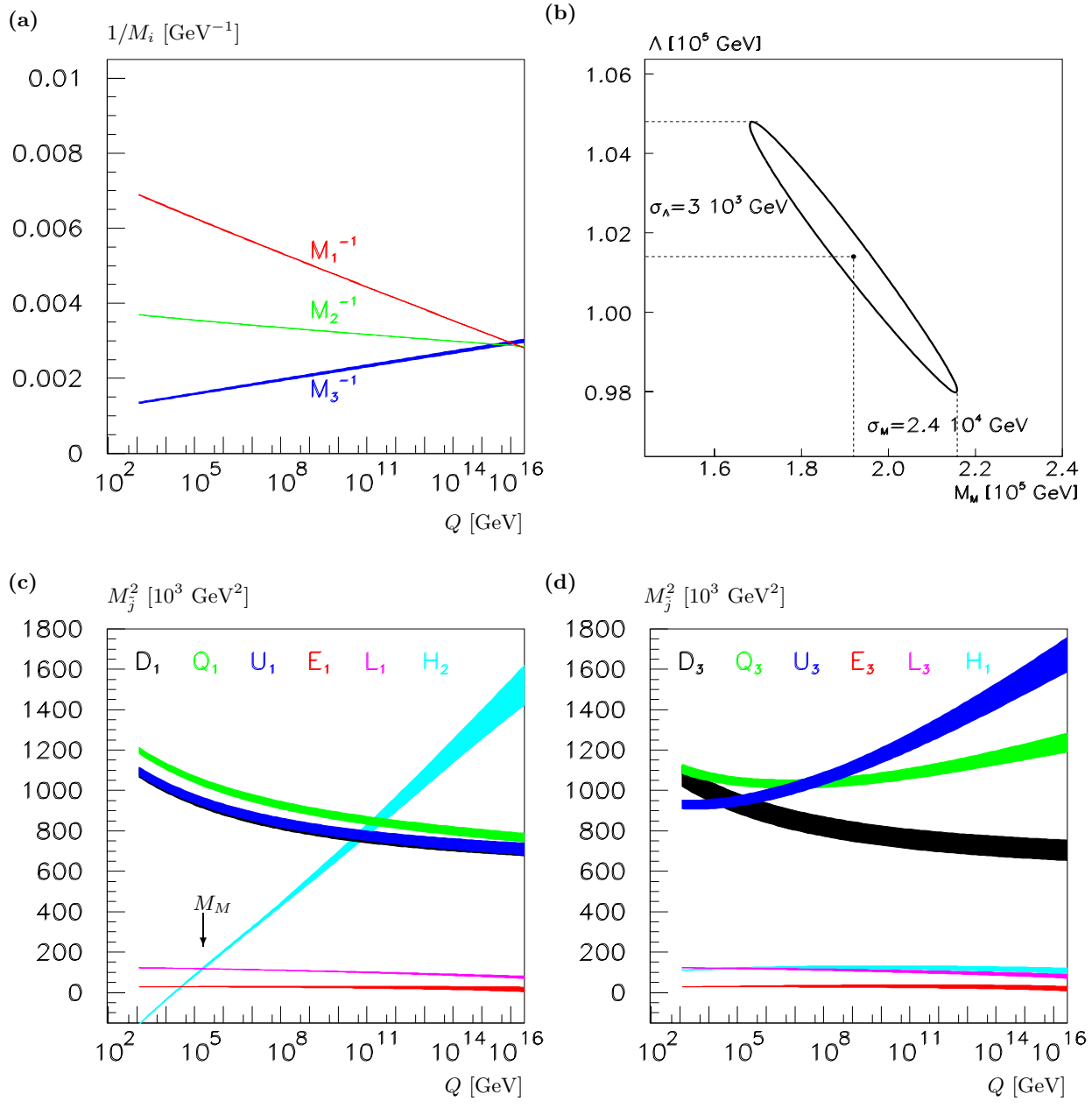

Fig. 4a–d. GMSB: Evolution of **a** gaugino mass parameters; **b** Λ-$M_{\rm M}$ determination in the bottom–up approach; **c** first-generation sfermion mass parameters and Higgs mass parameter $M_{H_2}^2$; **d** third-generation sfermion mass parameters and Higgs mass parameter $M_{H_1}^2$. The point probed, SPS#8, is characterized by the parameters $M_{\rm M} = 200\,\text{TeV}$, $\Lambda = 100\,\text{TeV}$, $N_5 = 1$, $\tan\beta = 15$, and $\text{sign}(\mu) = (+)$. [The widths of the bands indicate the 1σ CL.]

reconciled with the higher string scale by moduli dependent string loop corrections.

In the following we assume that all moduli fields get the same vacuum expectation values and that they couple in the same way to matter fields. Therefore, we omit the index m and take only one moduli field T.

The properties of the supersymmetric theories are quite different for dilaton and moduli dominated scenarios. This can be quantified by introducing a mixing angle θ, characterizing the $\tilde{S}$ and $\tilde{T}$ components in the wave functions of the Goldstino, which is associated with the breaking of supersymmetry and which is absorbed to generate the mass of the gravitino:

$$\tilde{G} = \sin\theta\tilde{S} + \cos\theta\tilde{T}. \tag{31}$$

The mass scale is set by the second parameter of the theory, the gravitino mass $m_{3/2}$.

A dilaton dominated scenario, i.e. $\sin\theta \to 1$, leads to universal boundary conditions of the soft supersymmetry breaking parameters. Universality is broken[8] only slightly

[8] For other mechanisms of breaking universality see e.g. [66]

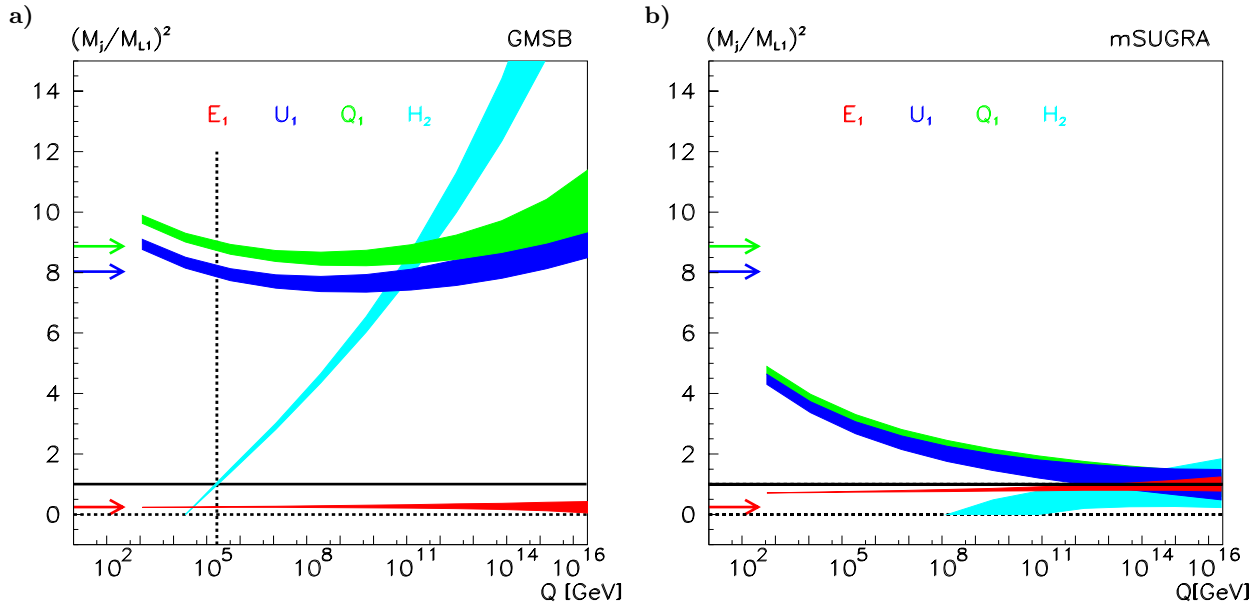

Fig. 5a,b. Evolution of representative ratios of first-generation scalar masses squared, **a** in case of GMSB; **b** in case of mSUGRA. The messenger scale $M_{\rm M}$ is defined as the scale where $M_{H_2} = M_{\rm L_1}$. The arrows in *both* figures indicate the expectation values of the mass ratios squared in GMSB at the scale $M_{\rm M}$

by small loop effects. On the other hand, in moduli field dominated scenarios, $\cos\theta \to 1$, the gaugino mass parameters are universal to lowest order [broken only in higher orders], but universality is not realized for the scalar mass parameters in general. The breaking is quantified by modular weights n_j characterizing the couplings between the matter and the moduli fields in orbifold compactifications. Within one generation significant differences between left and right field components and between sleptons and squarks can occur; since these patterns are modified only by small loop effects between different generations, flavor-changing neutral effects remain suppressed.

In leading order, and next-to-leading order denoted by the quantities ΔM, the masses [13] are given by the following expressions for the gaugino sector:

$$M_i = -g_i^2 m_{3/2} s\sqrt{3}\sin\theta + \Delta M_i, \tag{32}$$

$$\Delta M_i = -\frac{g_i^2}{16\pi^2} m_{3/2}\left\{ b_i + s\sqrt{3}\sin\theta g_s^2\left(C_i - \sum_j C_i^j\right) + 2t\cos\theta G_2(t)\left[\delta_{\rm GS} + b_i - 2\sum_j C_i^j(1+n_j)\right]\right\}, \tag{33}$$

and for the scalar sector

$$M_j^2 = m_{3/2}^2\left(1 + n_j\cos^2\theta\right) + \Delta M_j^2, \tag{34}$$

$$\Delta M_j^2 = m_{3/2}^2\left\{2\sqrt{3}s\sin\theta\left[\sum_i \gamma_j^i g_i^2 - \frac{1}{2s}\sum_{km}\gamma_j^{km}\right] + \gamma_j + 2t\cos\theta G_2(t)\sum_{km}\gamma_j^{km}(n_j + n_k + n_m + 3)\right\}, \tag{35}$$

while the A parameters read

$$A_{jkm} = -m_{3/2}\left[2t\cos\theta(n_j + n_k + n_m + 3)G_2(t) - \frac{\sin\theta}{\sqrt{3}}\right] + \Delta A_{jkm}, \tag{36}$$

$$\Delta A_{jkm} = m_{3/2}(\gamma_j + \gamma_k + \gamma_m). \tag{37}$$

The mass $m_{3/2}$ is the gravitino mass introduced earlier. The gravitino mass can be expressed in terms of the Kähler potential K and the superpotential W, which include the (non-perturbative) solutions of all the fields at the string scale: $m_{3/2} = \langle \exp(K/2)\overline{W}\rangle$. $s = \langle S\rangle$ is the vacuum expectation values of the dilaton field. $t = \langle T\rangle/m_{3/2}$ is the vacuum expectation value of the moduli field(s), and $G_2(t) = 2\zeta(t) + 1/2t$ is the non-holomorphic Eisenstein function with ζ denoting the Riemann zeta function. $\delta_{\rm GS}$ is the parameter of the Green–Schwarz counterterm. The γ_j are the anomalous dimensions of the matter fields, the γ_j^i and γ_j^{km} are their gauge and Yukawa parts, respectively. C_i, C_i^j are the quadratic Casimir operators for the gauge group G_i, respectively, in the adjoint representation and in the matter representation.

In the case of the gaugino mass parameters the next-to-leading order effects induce a splitting proportional to the β-functions b_i which is large enough to be "measured" at future collider experiments as demonstrated in Fig. 6a,b.

In the case of the scalar mass parameters the next-to-leading order contributions generate small departures from non-universality between the generations even if the corresponding modular weight is generation independent. These departures are proportional to the Yukawa couplings squared so that the third generation, in particular the stop sector, is mainly affected.

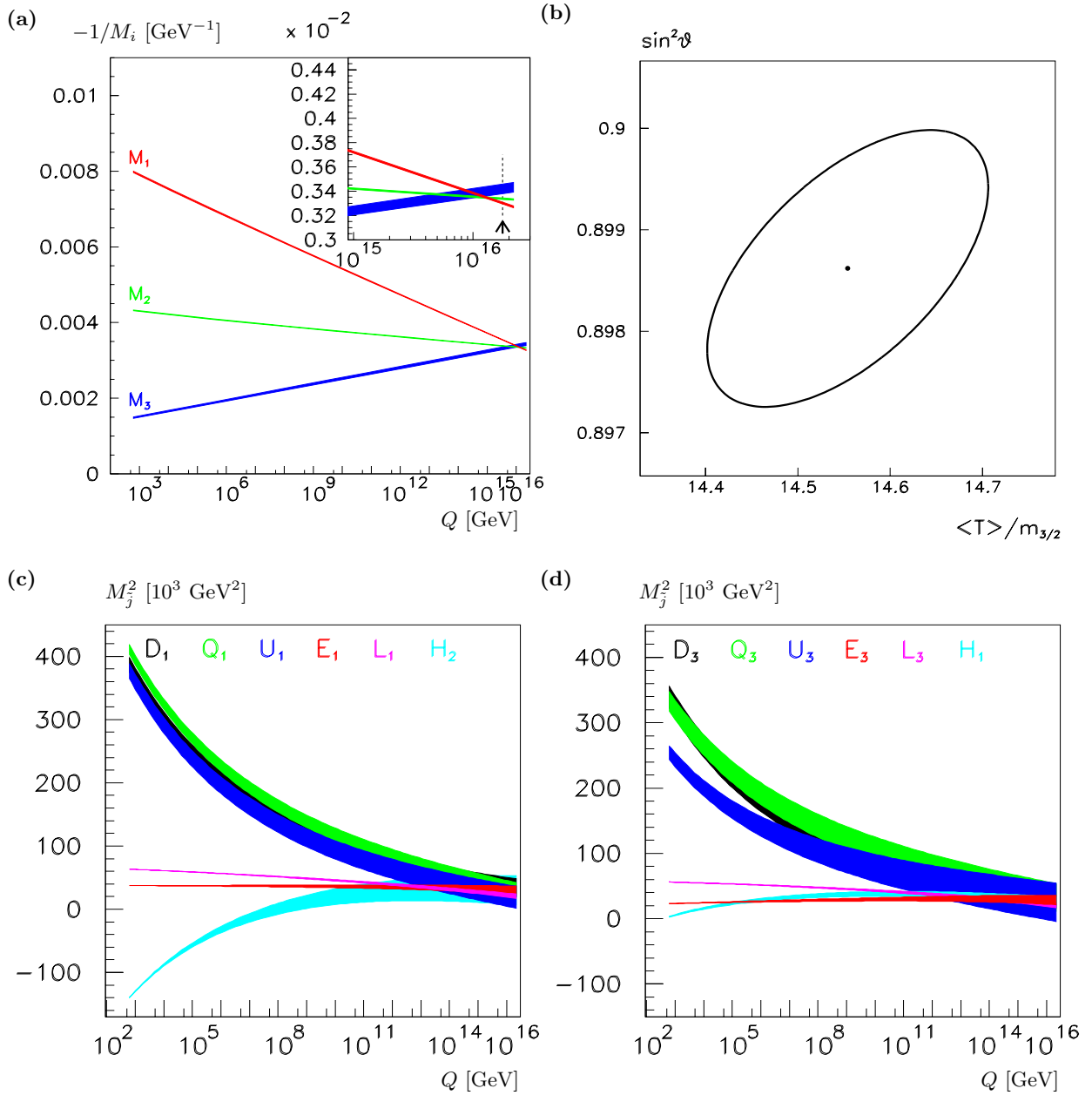

Fig. 6a,b. String scenario: Evolution of **a** gaugino mass parameters [the insert expands on the breaking of universality at the GUT scale]; **b** correlation between the mixing parameter $\sin^2\theta$ and the vacuum expectation value of the moduli field $\langle T\rangle$; **c** evolution of first-generation sfermion mass parameters and Higgs mass parameters $M_{H_2}^2$; **d** evolution of third-generation sfermion mass parameters and Higgs mass parameters $M_{H_1}^2$. The point probed is characterized by the parameters $m_{3/2} = 180\,\text{GeV}$, $\delta_{\text{GS}} = 0$, $\sin^2\theta = 0.9$, $< T >= 14\,m_{3/2}$, $\tan\beta = 10$, $\text{sign}(M_2\mu) = (+)$, $n_{L_i} = -3$, $n_{E_i} = -1$,$n_{Q_i} = 0$, $n_{U_i} = -2$, $n_{D_i} = 1$ and $n_{H_1} = n_{H_2} = -1$. [The widths of the bands indicate the 1σ CL.]

Scenarios have been found in which the phenomenological unification of the three gauge couplings can be reconciled with a string mass scale which is an order of magnitude larger than the unification scale [67]:

$$\alpha_i^{-1}(M_U) = \alpha^{-1}(M_{\text{String}}) + \Delta\alpha_i^{-1} \tag{38}$$

The corrections $\Delta\alpha_i^{-1}$ to universality at M_U depend on the value of the moduli fields and the modular weights:

$$\Delta\alpha_i^{-1} = \frac{1}{4\pi}(b_i' - b_{\text{GS}})\log|\eta(t)|^4, \tag{39}$$

where $\eta(t)$ is the Dedekind η-function and

$$b_3' = 9 + \sum_{i=1}^{3}(2n_{Q_i} + n_{U_i} + n_{D_i})\,, \tag{40}$$

Table 7. Representative gaugino / scalar mass parameters and couplings as determined at the electroweak scale and evolved to the GUT scale in the string scenario; based on LHC and LC simulations. $M^2_{\tilde{L}_{1,3}}$, $M^2_{\tilde{Q}_{1,3}}$ are the slepton and squark isodoublet parameters of the first and third family whereas $M^2_{\tilde{E}_{1,3}}$, $M^2_{\tilde{U}_{1,3}}$ and $M^2_{\tilde{D}_{1,3}}$ are the slepton and squark isosinglet parameters of the first and third family. [The errors quoted correspond to 1σ.]

	Exp. input	GUT value
M_1 [GeV]	-124.98 ± 0.29	-303.22 ± 0.65
M_2 [GeV]	-231.00 ± 0.50	-299.64 ± 0.52
M_3 [GeV]	-677.3 ± 7.6	-292.4 ± 3.3
μ	-377.59 ± 0.29	-375.5 ± 1.2
$M^2_{\tilde{L}_1}$ [GeV^2]	$(6.354 \pm 0.005) \cdot 10^4$	$(2.17 \pm 0.43) \cdot 10^4$
$M^2_{\tilde{E}_1}$ [GeV^2]	$(3.739 \pm 0.005) \cdot 10^4$	$(2.88 \pm 0.86) \cdot 10^4$
$M^2_{\tilde{Q}_1}$ [GeV^2]	$(4.16 \pm 0.09) \cdot 10^5$	$(3.1 \pm 1.3) \cdot 10^4$
$M^2_{\tilde{U}_1}$ [GeV^2]	$(3.80 \pm 0.12) \cdot 10^5$	$(2.5 \pm 1.9) \cdot 10^4$
$M^2_{\tilde{D}_1}$ [GeV^2]	$(3.88 \pm 0.13) \cdot 10^5$	$(3.5 \pm 1.7) \cdot 10^4$
$M^2_{\tilde{L}_3}$ [GeV^2]	$(5.635 \pm 0.039) \cdot 10^4$	$(2.18 \pm 0.46) \cdot 10^4$
$M^2_{\tilde{E}_3}$ [GeV^2]	$(2.253 \pm 0.024) \cdot 10^4$	$(2.90 \pm 0.93) \cdot 10^4$
$M^2_{\tilde{Q}_3}$ [GeV^2]	$(3.28 \pm 0.13) \cdot 10^5$	$(3.2 \pm 2.1) \cdot 10^4$
$M^2_{\tilde{U}_3}$ [GeV^2]	$(2.58 \pm 0.15) \cdot 10^5$	$(2.6 \pm 3.3) \cdot 10^4$
$M^2_{\tilde{D}_3}$ [GeV^2]	$(3.53 \pm 0.15) \cdot 10^5$	$(3.5 \pm 1.8) \cdot 10^4$
$M^2_{H_1}$ [GeV^2]	$(3.80 \pm 0.82) \cdot 10^3$	$(2.85 \pm 0.62) \cdot 10^4$
$M^2_{H_2}$ [GeV^2]	$(-1.429 \pm 0.004) \cdot 10^5$	$(3.1 \pm 2.7) \cdot 10^4$
A_t [GeV]	452 ± 17	-96 ± 64
$\tan\beta$	9.93 ± 0.88	–

$$b'_2 = 15 + \sum_{i=1}^{3} (3n_{Q_i} + n_{L_i}) + n_{H_1} + n_{H_2}, \tag{41}$$

$$b'_1 = \frac{99}{5} + \frac{1}{5} \sum_{i=1}^{3} (n_{Q_i} + 8n_{U_i} + 2n_{D_i} + 3n_{L_i} + 6n_{E_i}) + \frac{3}{5}(n_{H_1} + n_{H_2}) \tag{42}$$

as compared to the one-loop $SU(3) \times SU(2) \times U(1)$ β-functions $(b_3, b_2, b_1) = 33/5, 1, -3$.

We have analyzed a mixed dilaton / moduli superstring scenario but with dominating dilaton field component, $\sin^2\theta = 0.9$, and with different couplings of the moduli field to the (L,R) sleptons, the (L,R) squarks and to the Higgs fields, corresponding to the O-I representation $n_{L_i} = -3$, $n_{E_i} = -1$, $n_{H_1} = n_{H_2} = -1$, $n_{Q_i} = 0$, $n_{D_i} = 1$ and $n_{U_i} = -2$, that is one out of several assignments that is adopted quite frequently in the literature. The gravitino mass is chosen to be 180 GeV in this analysis.

We find for the low-energy data: $\mathrm{BR}(b \to s\gamma) = 3.1 \cdot 10^{-4}$, $\Delta[g-2]_\mu = 14 \cdot 10^{-10}$, $\Delta\rho = 13 \cdot 10^{-5}$; and $\Omega h^2 = 0.25$.

Given this set of superstring induced parameters, the evolution of the gaugino and scalar mass parameters is displayed in Fig. 6. The pattern of the trajectories is remarkably different from the other scenarios. The breaking of universality in the gaugino sector, induced by string threshold corrections, cf. Table 7, can be demonstrated at a statistically significant level.

Table 8. Comparison of the experimentally reconstructed values with the ideal fundamental parameters in a specific example for a string effective field theory

Parameter	Ideal	Reconstructed
$m_{3/2}$	180	179.9 ± 0.4
$\langle S \rangle$	2	1.998 ± 0.006
$\langle T \rangle$	14	14.6 ± 0.2
$\sin^2\theta$	0.9	0.899 ± 0.002
g_s^2	0.5	0.501 ± 0.002
δ_{GS}	0	0.1 ± 0.4
n_{L}	-3	-2.94 ± 0.04
n_E	-1	-1.00 ± 0.05
n_Q	0	0.02 ± 0.02
n_U	-2	-2.01 ± 0.02
n_D	$+1$	0.80 ± 0.04
n_{H_1}	-1	-0.96 ± 0.06
n_{H_2}	-1	-1.00 ± 0.02
$\tan\beta$	10	10.00 ± 0.13

In fact, these differences can be exploited to determine superstring parameters as argued above. The number of observables in the set of gauge couplings g_i, gaugino masses M_i and scalar masses $M_{\tilde{j}}$ exceeds the number of parameters in the superstring effective field theory: the gravitino mass $m_{3/2}$, the dilaton / moduli mixing angle $\sin\theta$, the ground-state value of the moduli field $\langle T \rangle$ and the ground-state value of the dilaton field $\langle S \rangle$. The latter is at tree level directly related to the string coupling: $1/g_s^2 = \langle S \rangle$.

Based on the "experimental" input observables, the fundamental parameters of the string effective field theory can be reconstructed; the reconstructed values are compared with the ideal values in Table 8. The errors for the basic parameters $\sin\theta$, $\langle T \rangle / m_{3/2}$ are displayed in Fig. 6b.

Thus, high-precision measurements at high energy proton and e^+e^- linear colliders provide access to crucial derivative parameters in string theories.

5 Conclusions

In supersymmetric theories stable extrapolations can be performed from the electroweak scale to the grand unification scale close to the Planck scale. This feature has been demonstrated compellingly in the evolution of the three gauge couplings to the unification point in the minimal supersymmetric theory.

Such extrapolations are made possible by high-precision measurements of the low-energy parameters. The operation of the e^+e^- colliders LEP and SLC has been crucial in this context. In the near future an enormous extension of this area will be possible if measurements

at LHC and prospective e^+e^- linear colliders are combined to draw, if realized in nature, a comprehensive high-precision picture of the supersymmetric particles and their interactions. Based merely on measurements at low energies, the parameters of the theory can be evolved to high scales by means of renormalization group techniques.

Supersymmetric theories and their breaking mechanisms have simple structures and great regularities at high scales. Extrapolations to high scales are therefore crucial to uncover the regularities. The bottom–up approach in the extrapolation of parameters measured at low scales to the high scales provides the most transparent picture. In this way the basis of the SUSY breaking mechanism can be explored and the crucial elements of the fundamental supersymmetric theory can be reconstructed. The method can thus be used to explore particle physics phenomena at a scale where, eventually, particle physics is linked to gravity.

Apart from other examples, we have focused on two interesting scenarios in this approach. The universality of gaugino and scalar mass parameters in minimal supergravity can be demonstrated very clearly if realized in the supersymmetric theory. Small deviations from universality, on the other hand, may be exploited to measure the fundamental parameters in superstring effective field theories, i.e. the strength of dilaton and moduli fields, their mixing and the modular weights. In this way, high-precision extrapolations of gauge and supersymmetry parameters can establish direct contact between superstring theory and experiment.

Many more refinements of the theoretical calculations and future experimental analyses will be necessary to expand the picture we have drawn in this first attempt. However, the prospect of exploring elements of the ultimate unification of the interactions provides a strong impetus to this direction.

Acknowledgements. We are very grateful for enlightening discussions with J. Kalinowski, G.L. Kane, B.D. Nelson and H.P. Nilles. G.A.B. is grateful for the hospitality extended to him in long-term visits to CERN and DESY, for support from the British Council ARC programme and Intas grant 00-00679. W.P. is supported by the Erwin Schrödinger fellowship No. J2095 of the "Fonds zur Förderung der wissenschaftlichen Forschung" of Austria FWF and partly by the Swiss "Nationalfonds".

Appendix

A One-loop RGEs

In this first appendix we collect the one-loop renormalization group equations (RGEs) including right-handed neutrinos.

Using the notation for the gauge and Yukawa couplings

$$\alpha_i = \frac{g_i^2}{16\pi^2},\ i=1,2,3; \quad Y_k = \frac{y_k^2}{16\pi^2},\ k = t,b,\tau,\nu, \tag{43}$$

the one-loop RG equations can be written as

$$\dot{\alpha}_i = -b_i\alpha_i^2, \tag{44}$$

$$\dot{Y}_k = Y_k\left(\sum_i c_{ki}\alpha_i - \sum_l a_{kl}Y_l\right), \tag{45}$$

where the dot denotes the derivative with respect to $t = \log M_U^2/Q^2$, and

$$b_i = \{33/5, 1, -3\}, \tag{46}$$

$$c_{ti} = \{13/15, 3, 16/3\}, \quad c_{bi} = \{7/15, 3, 16/3\}, \tag{47}$$

$$c_{\tau i} = \{9/5, 3, 0\}, \quad c_{\nu i} = \{3/5, 3, 0\}, \tag{48}$$

$$a_{tl} = \{6, 1, 0, 1\}, \quad a_{bl} = \{1, 6, 1, 0\}, \tag{49}$$

$$a_{\tau l} = \{0, 3, 4, 1\}, \quad a_{\nu l} = \{3, 0, 1, 4\}, \tag{50}$$

while the RGEs for the gaugino mass parameters and the A parameters read

$$\dot{M}_i = -b_i\alpha_i M_i, \tag{51}$$

$$\dot{A}_k = \sum_i c_{ki}\alpha_i M_i - \sum_l a_{kl}A_l. \tag{52}$$

The RGEs for the soft SUSY breaking mass parameters of the third generation and the Higgs mass parameters are given by

$$\dot{M}_{\tilde{L}_3} = -2Y_\tau X_\tau - 2Y_\nu X_\nu + \frac{6}{5}\alpha_1 M_1^2 + 6\alpha_2 M_2^2 + \frac{3}{5}S, \tag{53}$$

$$\dot{M}_{\tilde{N}_3} = -4Y_\nu X_\nu, \tag{54}$$

$$\dot{M}_{\tilde{E}_3} = -4Y_\tau X_\tau + \frac{24}{5}\alpha_1 M_1^2 - \frac{6}{5}S, \tag{55}$$

$$\dot{M}_{\tilde{Q}_3} = -2Y_b X_b - 2Y_t X_t + \frac{2}{15}\alpha_1 M_1^2 + 6\alpha_2 M_2^2 + \frac{16}{3}\alpha_3 M_3^2 - \frac{1}{5}S, \tag{56}$$

$$\dot{M}_{\tilde{U}_3} = -4Y_t X_t + \frac{32}{15}\alpha_1 M_1^2 + \frac{16}{3}\alpha_3 M_3^2 + \frac{4}{5}S, \tag{57}$$

$$\dot{M}_{\tilde{D}_3} = -4Y_b X_b + \frac{8}{15}\alpha_1 M_1^2 + \frac{16}{3}\alpha_3 M_3^2 - \frac{2}{5}S, \tag{58}$$

$$\dot{M}_{H_1} = -6Y_b X_b - 2Y_\tau X_\tau + \frac{6}{5}\alpha_1 M_1^2 + 6\alpha_2 M_2^2 + \frac{3}{5}S, \tag{59}$$

$$\dot{M}_{H_2} = -6Y_t X_t - 2Y_\nu X_\nu + \frac{6}{5}\alpha_1 M_1^2 + 6\alpha_2 M_2^2 - \frac{3}{5}S, \tag{60}$$

with

$$X_t = M_{\tilde{Q}_3}^2 + M_{\tilde{U}_3}^2 + M_{H_2}^2 + A_t^2, \tag{61}$$

$$X_b = M_{\tilde{Q}_3}^2 + M_{\tilde{D}_3}^2 + M_{H_1}^2 + A_b^2, \tag{62}$$

$$X_\tau = M_{\tilde{L}_3}^2 + M_{\tilde{E}_3}^2 + M_{H_1}^2 + A_\tau^2, \tag{63}$$

$$X_\nu = M_{\tilde{L}_3}^2 + M_{\tilde{N}_3}^2 + M_{H_2}^2 + A_\nu^2, \tag{64}$$

$$S = M_{H_2}^2 - M_{H_1}^2 + \sum_{i=1}^{3}\left(M_{\tilde{Q}_i}^2 - M_{\tilde{L}_i}^2 - 2M_{\tilde{U}_i}^2 + M_{\tilde{D}_i}^2 + M_{\tilde{E}_i}^2\right). \quad (65)$$

The evolution equations for the first two generations are obtained by replacing appropriately the corresponding parameters and Yukawa couplings.

B Solutions of the one-loop RGEs

In the following subsections we present the analytical solutions to the one-loop RGEs including Yukawa couplings using the procedure of [68]. We also include the generic trace term S (see (65)) in the solutions which had been neglected in [68].

In this appendix we mark all quantities defined at the GUT-scale M_U with a subscript U.

B.1 MSUGRA boundary conditions at the GUT scale

The solutions for the case of the MSSM are summarized first for proper reference.

The solution for the gauge couplings and Yukawa couplings are given by

$$\alpha_i(t) = \frac{\alpha_{i,U}}{1 + b_i \alpha_{i,U} t}, \quad (66)$$

$$Y_k(t) = \frac{Y_{k,U} u_k}{1 + a_{kk} Y_{k,U} \int_0^t u_k}, \quad (67)$$

where the functions u_k obey the integral system of equations

$$u_t = \frac{E_t}{(1 + 6Y_{b,U} \int_0^t u_b)^{1/6}}, \quad (68)$$

$$u_b = \frac{E_b}{(1 + 6Y_{t,U} \int_0^t u_t)^{1/6} (1 + 4Y_{\tau,U} \int_0^t u_\tau)^{1/4}}, \quad (69)$$

$$u_\tau = \frac{E_\tau}{(1 + 6Y_{b,U} \int_0^t u_b)^{1/2}}, \quad (70)$$

and the functions E_k denote the products

$$E_k = \prod_{i=1}^{3} (1 + b_i \alpha_{i,U} t)^{c_{ki}/b_i}. \quad (71)$$

The system of integral equations can be solved iteratively and a discussion on the convergence can be found in [68].

The gaugino mass parameters and the A_k parameters are given by

$$M_i(t) = \frac{M_{i,U}}{1 + b_i \alpha_{i,U} t} = \frac{\alpha_i(t)}{\alpha_{i,U}} M_{i,U}, \quad (72)$$

$$A_k = -e_k + \frac{A_{k,U}/Y_{k,U} + a_{kk} \int u_k e_k}{1/Y_{k,U} + a_{kk} \int u_k}, \quad (73)$$

with the coefficients

$$e_t = \tilde{F}_t + \frac{A_{b,U} \int u_b - \int u_b e_b}{1/Y_{b,U} + 6 \int u_b}, \quad (74)$$

$$e_b = \tilde{F}_b + \frac{A_{t,U} \int u_t - \int u_t e_t}{1/Y_{t,U} + 6 \int u_t} + \frac{A_{\tau,U} \int u_\tau - \int u_\tau e_\tau}{1/Y_{\tau,U} + 4 \int u_\tau}, \quad (75)$$

$$e_\tau = \tilde{F}_\tau + 3 \frac{A_{b,U} \int u_b - \int u_b e_b}{1/Y_{b,U} + 6 \int u_b}, \quad (76)$$

$$\tilde{F}_k = t \sum_{i=1}^{3} c_{ki} M_{i,U} \alpha_i(t). \quad (77)$$

The mass parameters of the first two generations ($k = 1, 2$) can be expressed as

$$M_{\tilde{L}_k}^2(t) = M_{\tilde{L}_k,U}^2 + \frac{3}{2} f_2(t) + \frac{3}{10} f_1(t) + \frac{3}{5} S'(t), \quad (78)$$

$$M_{\tilde{E}_k}^2(t) = M_{\tilde{E}_k,U}^2 + \frac{6}{5} f_1(t) - \frac{6}{5} S'(t), \quad (79)$$

$$M_{\tilde{Q}_k}^2(t) = M_{\tilde{Q}_k,U}^2 + \frac{8}{3} f_3(t) + \frac{3}{2} f_2(t) + \frac{1}{30} f_1(t) - \frac{1}{5} S'(t), \quad (80)$$

$$M_{\tilde{U}_k}^2(t) = M_{\tilde{U}_k,U}^2 + \frac{8}{3} f_3(t) + \frac{8}{15} f_1(t) + \frac{4}{5} S'(t), \quad (81)$$

$$M_{\tilde{D}_k}^2(t) = M_{\tilde{D}_k,U}^2 + \frac{8}{3} f_3(t) + \frac{2}{15} f_1(t) - \frac{2}{5} S'(t), \quad (82)$$

with

$$f_i(t) = \frac{M_{i,U}^2}{b_i} \left(1 - \frac{1}{(1 + \alpha_{i,U} b_i t)^2}\right), \quad (83)$$

$$S'(t) = \frac{1}{2b_1} \left[S(t) - S(M_U)\right], \quad (84)$$

$$S(t) = S(M_U)(1 + \beta_1 t)^2, \quad (85)$$

$$S(M_U) = M_{H_2,U}^2 - M_{H_1,U}^2 + \sum_{i=1}^{3} \left(M_{\tilde{Q}_i,U}^2 - M_{\tilde{L}_i,U}^2 - 2M_{\tilde{U}_i,U}^2 + M_{\tilde{D}_i,U}^2 + M_{\tilde{E}_i,U}^2\right), \quad (86)$$

in agreement with [69]. The mass parameters for the third generation and the Higgs mass parameters are involved owing to the Yukawa couplings:

$$M_{\tilde{L}_3}^2 = M_{\tilde{L}_3,U}^2 + \frac{80 f_3 + 123 f_2 - 103/5 f_1}{122} - \frac{3}{5} S'(t) + \frac{3\Delta\Sigma_t - 18\Delta\Sigma_b + 35\Delta\Sigma_\tau}{122}, \quad (87)$$

$$M_{\tilde{E}_3}^2 = M_{\tilde{E}_3,U}^2 + \frac{80 f_3 - 60 f_2 + 16 f_1}{61} + \frac{6}{5} S'(t) + \frac{3\Delta\Sigma_t - 18\Delta\Sigma_b + 35\Delta\Sigma_\tau}{61}, \quad (88)$$

$$M_{\tilde{Q}_3}^2 = M_{\tilde{Q}_3,U}^2 + \frac{128 f_3 + 87 f_2 - 11 f_1}{122} + \frac{1}{5} S'(t)$$

$$+\frac{17\Delta\Sigma_t+20\Delta\Sigma_b-5\Delta\Sigma_\tau}{122}, \quad (89)$$

$$M^2_{\tilde{U}_3}=M^2_{\tilde{U}_3,U}+\frac{72f_3-54f_2+72/5f_1}{61}-\frac{4}{5}S'(t)+\frac{21\Delta\Sigma_t-4\Delta\Sigma_b+\Delta\Sigma_\tau}{61}, \quad (90)$$

$$M^2_{\tilde{D}_3}=M^2_{\tilde{D}_3,U}+\frac{56f_3-42f_2+56/5f_1}{61}+\frac{2}{5}S'(t)+\frac{-4\Delta\Sigma_t+24\Delta\Sigma_b-6\Delta\Sigma_\tau}{61}, \quad (91)$$

$$M^2_{H_1}=M^2_{H_1,U}+\frac{-240f_3-3f_2-57/5f_1}{122}-\frac{3}{5}S'(t)+\frac{-9\Delta\Sigma_t+54\Delta\Sigma_b+17\Delta\Sigma_\tau}{122}, \quad (92)$$

$$M^2_{H_2}=M^2_{H_2,U}+\frac{-272f_3+21f_2-89/5f_1}{122}+\frac{3}{5}S'(t)+\frac{63\Delta\Sigma_t-12\Delta\Sigma_b+3\Delta\Sigma_\tau}{122}, \quad (93)$$

with

$$\Delta\Sigma_k=\Sigma_k(t)-\Sigma_{k,U}, \quad (94)$$

$$\Sigma_t=M^2_{\tilde{Q}_3}+M^2_{\tilde{U}_3}+M^2_{H_2}, \quad (95)$$

$$\Sigma_b=M^2_{\tilde{Q}_3}+M^2_{\tilde{D}_3}+M^2_{H1}, \quad (96)$$

$$\Sigma_\tau=M^2_{\tilde{L}_3}+M^2_{\tilde{E}_3}+M^2_{H1}. \quad (97)$$

The explicit solution for Σ_k reads

$$\Sigma_k=\xi_k+A_k^2+2e_kA_k-\frac{A^2_{k,U}/Y_{k,U}-\Sigma_{k,U}/Y_{k,U}+a_{kk}\int u_k\xi_k}{1/Y_{k,U}+a_{kk}\int u_k}, \quad (98)$$

with

$$\xi_t=\tilde{E}_t+2\tilde{F}_t\frac{A_{b,U}\int u_b-\int u_be_b}{1/Y_{b,U}+6\int u_b} \quad (99)$$
$$+7\left(\frac{A_{b,U}\int u_b-\int u_be_b}{1/Y_{b,U}+6\int u_b}\right)^2$$
$$-\frac{(\Sigma_{b,U}+A^2_{b,U})\int u_b-2A_{b,U}\int u_be_b+\int u_b\xi_b}{1/Y_{b,U}+6\int u_b},$$

$$\xi_b=\tilde{E}_b \quad (100)$$
$$+2\tilde{F}_b\left[\frac{A_{t,U}\int u_t-\int u_te_t}{1/Y_{t,U}+6\int u_t}+\frac{A_{\tau,U}\int u_\tau-\int u_\tau e_\tau}{1/Y_{\tau,U}+4\int u_\tau}\right]$$
$$+7\left(\frac{A_{t,U}\int u_t-\int u_te_t}{1/Y_{t,U}+6\int u_t}\right)^2$$
$$+5\left(\frac{A_{\tau,U}\int u_\tau-\int u_\tau e_\tau}{1/Y_{\tau,U}+4\int u_\tau}\right)^2$$
$$+2\left(\frac{A_{t,U}\int u_t-\int u_te_t}{1/Y_{t,U}+6\int u_t}\right)\left(\frac{A_{\tau,U}\int u_\tau-\int u_\tau e_\tau}{1/Y_{\tau,U}+4\int u_\tau}\right)$$
$$-\frac{(\Sigma_{t,U}+A^2_{t,U})\int u_t-2A_{t,U}\int u_te_t+\int u_t\xi_t}{1/Y_{t,U}+6\int u_t}$$
$$-\frac{(\Sigma_{\tau,U}+A^2_{\tau,U})\int u_\tau-2A_{\tau,U}\int u_\tau e_\tau+\int u_\tau\xi_\tau}{1/Y_{\tau,U}+4\int u_\tau},$$

$$\xi_\tau=\tilde{E}_\tau+6\tilde{F}_\tau\frac{A_{b,U}\int u_b-\int u_be_b}{1/Y_{b,U}+6\int u_b} \quad (101)$$
$$+27\left(\frac{A_{b,U}\int u_b-\int u_be_b}{1/Y_{b,U}+6\int u_b}\right)^2$$
$$-3\frac{(\Sigma_{b,U}+A^2_{b,U})\int u_b-2A_{b,U}\int u_be_b+\int u_b\xi_b}{1/Y_{b,U}+6\int u_b},$$

$$\tilde{E}_k=t^2\left(\sum_{i=1}^3c_{ki}\alpha_iM_{i,U}\right)^2+2t\sum_{i=1}^3c_{ki}\alpha_iM^2_{i,U} \quad (102)$$
$$-t^2\sum_{i=1}^3c_{ki}b_i\alpha_i^2M^2_{i,U}.$$

Finally we express $t_Z=\log(M_U^2/m_Z^2)$ and α_U in terms of observables at the electroweak scale, using (66), by

$$t_Z=\frac{4\pi}{(b_1-b_2)\alpha(m_Z)}\left(\frac{3\cos^2\vartheta_{\rm W}}{5}-\sin^2\vartheta_{\rm W}\right), \quad (103)$$

and similarly for the gauge coupling at the GUT scale:

$$\alpha_U=\frac{5\alpha(m_Z)}{3}\frac{b_1-b_2}{\frac{5}{3}b_1\sin^2\Theta_{\rm W}-b_2\cos^2\Theta_{\rm W}}. \quad (104)$$

B.2 Universal SUGRA boundary conditions at the GUT scale including right-handed neutrinos

Those formulae are noted in this subsection which are changed compared to the previous section in the range between M_U and $M_{\nu_{\rm R}}$. Below $M_{\nu_{\rm R}}$, these quantities have the same form as given above. In addition we note also the equations related to the right-handed neutrinos:

$$u_t=\frac{E_t}{(1+6Y_{b,U}\int_0^t u_b)^{1/6}(1+4Y_{\nu,U}\int_0^t u_\nu)^{1/4}}, \quad (105)$$

$$u_\tau=\frac{E_\tau}{(1+6Y_{b,U}\int_0^t u_b)^{1/2}(1+4Y_{\nu,U}\int_0^t u_\nu)^{1/4}}, \quad (106)$$

$$u_\nu=\frac{E_\nu}{(1+6Y_{t,U}\int_0^t u_t)^{1/2}(1+4Y_{\tau,U}\int_0^t u_\tau)^{1/4}}, \quad (107)$$

$$e_t=\tilde{F}_t+\frac{A_{b,U}\int u_b-\int u_be_b}{1/Y_{b,U}+6\int u_b}+\frac{A_{\nu,U}\int u_\nu-\int u_\nu e_\nu}{1/Y_{\nu,U}+4\int u_\nu}, \quad (108)$$

$$e_\tau=\tilde{F}_\tau+3\frac{A_{b,U}\int u_b-\int u_be_b}{1/Y_{b,U}+6\int u_b}+\frac{A_{\nu,U}\int u_\nu-\int u_\nu e_\nu}{1/Y_{\nu,U}+4\int u_\nu}, \quad (109)$$

$$e_\nu=\tilde{F}_\nu+3\frac{A_{t,U}\int u_t-\int u_te_t}{1/Y_{t,U}+6\int u_t}+\frac{A_{\tau,U}\int u_\tau-\int u_\tau e_\tau}{1/Y_{\tau,U}+4\int u_\tau}. \quad (110)$$

$$\xi_t=\tilde{E}_t+2\tilde{F}_t\left(\frac{A_{b,U}\int u_b-\int u_be_b}{1/Y_{b,U}+6\int u_b}+\frac{A_{\nu,U}\int u_\nu-\int u_\nu e_\nu}{1/Y_{\nu,U}+4\int u_\nu}\right)$$

$$
\begin{aligned}
&+ 7\left(\frac{A_{b,U}\int u_b - \int u_b e_b}{1/Y_{b,U} + 6\int u_b}\right)^2 \\
&+ 5\left(\frac{A_{\nu,U}\int u_\nu - \int u_\nu e_\nu}{1/Y_{\nu,U} + 4\int u_\nu}\right)^2 \\
&+ 2\left(\frac{A_{b,U}\int u_b - \int u_b e_b}{1/Y_{b,U} + 6\int u_b}\right)\left(\frac{A_{\nu,U}\int u_\nu - \int u_\nu e_\nu}{1/Y_{\nu,U} + 4\int u_\nu}\right) \\
&- \frac{(\Sigma_{b,U} + A_{b,U}^2)\int u_b - 2A_{b,U}\int u_b e_b + \int u_b \xi_b}{1/Y_{b,U} + 6\int u_b}, \\
&- \frac{(\Sigma_{\nu,U} + A_{\nu,U}^2)\int u_\nu - 2A_{\nu,U}\int u_\nu e_\nu + \int u_\nu \xi_\nu}{1/Y_{\nu,U} + 4\int u_\nu},
\end{aligned}
\tag{111}
$$

$$
\begin{aligned}
\xi_\tau = {} & \tilde{E}_\tau \\
&+ 2\tilde{F}_\tau\left(3\frac{A_{b,U}\int u_b - \int u_b e_b}{1/Y_{b,U} + 6\int u_b} + \frac{A_{\nu,U}\int u_\nu - \int u_\nu e_\nu}{1/Y_{\nu,U} + 4\int u_\nu}\right) \\
&+ 27\left(\frac{A_{b,U}\int u_b - \int u_b e_b}{1/Y_{b,U} + 6\int u_b}\right)^2 \\
&+ 5\left(\frac{A_{\nu,U}\int u_\nu - \int u_\nu e_\nu}{1/Y_{\nu,U} + 4\int u_\nu}\right)^2 \\
&+ 6\left(\frac{A_{b,U}\int u_b - \int u_b e_b}{1/Y_{b,U} + 6\int u_b}\right)\left(\frac{A_{\nu,U}\int u_\nu - \int u_\nu e_\nu}{1/Y_{\nu,U} + 4\int u_\nu}\right) \\
&- 3\frac{(\Sigma_{b,U} + A_{b,U}^2)\int u_b - 2A_{b,U}\int u_b e_b + \int u_b \xi_b}{1/Y_{b,U} + 6\int u_b} \\
&- \frac{(\Sigma_{\nu,U} + A_{\nu,U}^2)\int u_\nu - 2A_{\nu,U}\int u_\nu e_\nu + \int u_\nu \xi_\nu}{1/Y_{\nu,U} + 4\int u_\nu},
\end{aligned}
\tag{112}
$$

$$
\begin{aligned}
\xi_\nu = {} & \tilde{E}_\nu \\
&+ 2\tilde{F}_\nu\left(3\frac{A_{t,U}\int u_t - \int u_t e_t}{1/Y_{t,U} + 6\int u_t} + \frac{A_{\tau,U}\int u_\tau - \int u_\tau e_\tau}{1/Y_{\tau,U} + 4\int u_\tau}\right) \\
&+ 27\left(\frac{A_{t,U}\int u_t - \int u_t e_t}{1/Y_{t,U} + 6\int u_t}\right)^2 \\
&+ 5\left(\frac{A_{\tau,U}\int u_\tau - \int u_\tau e_\tau}{1/Y_{\tau,U} + 4\int u_\tau}\right)^2 \\
&+ 6\left(\frac{A_{t,U}\int u_t - \int u_t e_t}{1/Y_{t,U} + 6\int u_t}\right)\left(\frac{A_{\tau,U}\int u_\tau - \int u_\tau e_\tau}{1/Y_{\tau,U} + 4\int u_\tau}\right) \\
&- 3\frac{(\Sigma_{t,U} + A_{t,U}^2)\int u_t - 2A_{t,U}\int u_t e_t + \int u_t \xi_t}{1/Y_{t,U} + 6\int u_t} \\
&- \frac{(\Sigma_{\tau,U} + A_{\tau,U}^2)\int u_\tau - 2A_{\tau,U}\int u_\tau e_\tau + \int u_\tau \xi_\tau}{1/Y_{\tau,U} + 4\int u_\tau};
\end{aligned}
\tag{113}
$$

$$
\Sigma_\nu = M_{\tilde{L}_3}^2 + M_{\tilde{N}_3}^2 + M_{H_2}^2. \tag{114}
$$

References

1. J. Wess, B. Zumino, Nucl. Phys. B **70**, 39 (1974); P. Fayet, S. Ferrara, Phys. Rept. **32**, 249 (1977)
2. H.P. Nilles, Phys. Rept. **110**, 1 (1984); H.E. Haber, G.L. Kane, Phys. Rept. **117**, 75 (1985)
3. E. Witten, Nucl. Phys. B **188**, 513 (1981)
4. S. Dimopoulos, S. Raby, F. Wilczek, Phys. Rev. D **24**, 1681 (1981); L.E. Ibáñez, G.G. Ross, Phys. Lett. B **105**, 439 (1981); U. Amaldi, W. de Boer, H. Fürstenau, Phys. Lett. B **260**, 447 (1991); P. Langacker, M. Luo, Phys. Rev. D **44**, 817 (1991); J. Ellis, S. Kelley, D.V. Nanopoulos, Phys. Lett. B **260**, 161 (1991)
5. L.E. Ibáñez, G.G. Ross, Phys. Lett. B **110**, 215 (1982)
6. J.R. Ellis, J.S. Hagelin, D.V. Nanopoulos, K.A. Olive, M. Srednicki, Nucl. Phys. B **238**, 453 (1984)
7. D.Z. Freedman, P. van Nieuwenhuizen, S. Ferrara, Phys. Rev. D **13**, 3214 (1976); S. Deser, B. Zumino, Phys. Lett. B **62**, 335 (1976)
8. A.H. Chamseddine, R. Arnowitt, P. Nath, Phys. Rev. Lett. **49**, 970 (1982)
9. M. Dine, A.E. Nelson, Phys. Rev. D **48**, 1277 (1993)
10. G.F. Giudice, M.A. Luty, H. Murayama, R. Rattazzi, JHEP **9812**, 027 (1998); L. Randall, R. Sundrum, Nucl. Phys. B **557**, 79 (1999)
11. D.E. Kaplan, G.D. Kribs, M. Schmaltz, Phys. Rev. D **62**, 035010 (2000); Z. Chacko, M.A. Luty, A.E. Nelson, E. Ponton, JHEP **0001**, 003 (2000)
12. M. Cvetič, A. Font, L.E. Ibáñez, D. Lüst, F. Quevedo, Nucl. Phys. B **361**, 194 (1991); A. Brignole, L.E. Ibáñez, C. Muñoz, Nucl. Phys. B **422**, 125 (1994) [Erratum ibid. B **436**, 747 (1995)]; A. Love, P. Stadler, Nucl. Phys. B **515**, 34 (1998)
13. P. Binetruy, M.K. Gaillard, B.D. Nelson, Nucl. Phys. B **604**, 32 (2001)
14. G.A. Blair, W. Porod, P.M. Zerwas, Phys. Rev. D **63**, 017703 (2001)
15. I. Hinchliffe et al., Phys. Rev. D **55**, 5520 (1997); Atlas Collaboration, Technical Design Report 1999, Vol. II, CERN/LHC/99-15, ATLAS TDR 15
16. P.M. Zerwas, Proceedings, 1999 Cargèse Institute for High-Energy Physics, hep-ph/0003221; H. Murayama, M.E. Peskin, Ann. Rev. Nucl. Part. Sci. **46**, 533 (1996); E. Accomando et al., ECFA/DESY LC Working Group, Phys. Rep. **299**, 1 (1998)
17. TESLA Technical Design Report, Part III: Physics at an e^+e^- Linear Collider, edited by R. Heuer, D.J. Miller, F. Richard, P.M. Zerwas [ECFA/DESY LC Physics Working Group Collaboration], DESY 01-110, hep-ph/0106315
18. B.C. Allanach et al., in Proceedings of the APS/DPF/DPB Summer Study on the Future of Particle Physics (Snowmass 2001), edited by R. Davidson, C. Quigg, Eur. Phys. J. C **25**, 113 (2002)
19. T.E. Clark, T.K. Kuo, N. Nakagawa, Phys. Lett. B **115**, 26 (1982); L.E. Ibáñez, Phys. Lett. B **114**, 243 (1982); Z.Y. Zhao, Nucl. Phys. B **212**, 224 (1983); C.S. Aulakh, R.N. Mohapatra, Phys. Rev. D **28**, 217 (1983)
20. M. Gell-Mann, P. Ramond, R. Slansky, in Supergravity, edited by F. van Nieuwenhuizen, D. Freedman (North Holland 1979); T. Yanagida, Proceedings, Unified Theory and the Baryon Number in the Universe, KEK 1979; R.N. Mohapatra, G. Senjanovic, Phys. Rev. Lett. **44**, 912 (1980)
21. E. Witten, Phys. Lett. B **155**, 151 (1985)
22. E. Witten, Talk at the Workshop on the Future of Particle Physics, Snowmass 2001
23. G.L. Kane, Proceedings of SUSY02, DESY Hamburg, http://www.desy.de/susy02/ and hep-ph/0210352

24. M.M. Nojiri, K. Fujii, T. Tsukamoto, Phys. Rev. D **54**, 6756 (1996)
25. G.A. Blair, U. Martyn, Proceedings, LC Workshop, Sitges 1999, hep-ph/9910416
26. M. Battaglia, Physics Signatures at CLIC, hep-ph/0103338
27. S. Ferrara, L. Girardello, F. Palumbo, Phys. Rev. D **20**, 403 (1979)
28. J. Hisano, H. Murayama, Phys. Rev. D **49**, 1446 (1994)
29. K. Inoue, A. Kakuto, H. Komatsu, S. Takeshita, Prog. Theor. Phys. **68**, 927 (1982); [Erratum **70**, 330 (1983)]
30. S. Martin, M. Vaughn, Phys. Rev. D **50**, 2282 (1994); Y. Yamada, Phys. Rev. D **50**, 3537 (1994); I. Jack, D.R.T. Jones, Phys. Lett. B **333**, 372 (1994)
31. J. Bagger, K. Matchev, D. Pierce, R. Zhang, Nucl. Phys. B **491**, 3 (1997)
32. S.Y. Choi, A. Djouadi, M. Guchait, J. Kalinowski, H.S. Song, P.M. Zerwas, Eur. Phys. J. C **14**, 535 (2000); S.Y. Choi, J. Kalinowski, G. Moortgat-Pick, P.M. Zerwas, Eur. Phys. J. C **22**, 563 (2001) [Addendum ibid. C **23**, 769 (2002)]
33. J.L. Feng, T. Moroi, Phys. Rev. D **56**, 5692 (1997); J.F. Gunion, T. Han, J. Jiang, S. Mrenna, A. Sopczak, in Proceedings of the APS/DPF/DPB Summer Study on the Future of Particle Physics (Snowmass 2001), edited by R. Davidson, C. Quigg, hep-ph/0112334
34. A. Bartl, K. Hidaka, T. Kernreiter, W. Porod, Phys. Rev. D **66**, 115009 (2002)
35. A. Bartl, H. Eberl, S. Kraml, W. Majerotto, W. Porod, A. Sopczak, Z. Phys. C **76**, 549 (1997); A. Bartl, H. Eberl, S. Kraml, W. Majerotto, W. Porod, Eur. Phys. J. direct C **6**, 1 (2000)
36. G. Degrassi, P. Slavich, F. Zwirner, Nucl. Phys. B **611**, 403 (2001); A. Brignole, G. Degrassi, P. Slavich, F. Zwirner, Nucl. Phys. B **631**, 195 (2002)
37. H. Arason et al., Phys. Rev. D **46**, 3945 (1992)
38. J.R. Primack, astro-ph/0205391
39. A.L. Kagan, M. Neubert, Eur. Phys. J. C **7**, 5 (1999); A. Ali, D. London, Phys. Rept. **320**, 79 (1999); D.A. Demir, A. Masiero, O. Vives, Phys. Rev. D **61**, 075009 (2000)
40. T. Ibrahim, P. Nath, Phys. Rev. D **61**, 095008 (2000)
41. M. Drees, K. Hagiwara, Phys. Rev. D **42**, 1709 (1990)
42. P. Gondolo et al., program DarkSusy, http://www.physto.se/~edsjo/darksusy
43. J.L. Feng, D.E. Finnell, Phys. Rev. D **49**, 2369 (1994); A. Bartl, H. Eberl, S. Kraml, W. Majerotto, W. Porod, EPJ direct C **6**, 1 (2000)
44. J.A. Casas, A. Lleyda, C. Muñoz, Nucl. Phys. B **471**, 3 (1996)
45. S. Weinberg, Phys. Lett. B **91**, 51 (1980)
46. L.J. Hall, Nucl. Phys. B **178**, 75 (1981)
47. G.G. Ross, R.G. Roberts, Nucl. Phys. B **377**, 571 (1992)
48. P. Langacker, N. Polonsky, Phys. Rev. D **47**, 4028 (1993)
49. M. Bastero-Gil, J. Perez-Mercader, Phys. Lett. B **322**, 355 (1994); M. Bastero-Gil, J. Perez-Mercader, Nucl. Phys. B **450**, 21 (1995)
50. A. Dedes, A.B. Lahanas, J. Rizos, K. Tamvakis, Phys. Rev. D **55**, 2955 (1997)
51. H. Murayama, A. Pierce, Phys. Rev. D **65**, 055009 (2002)
52. D.E. Groom et al. [Particle Data Group Collaboration], Eur. Phys. J. C **15**, 1 (2000)
53. K. Mönig, in Physics and Experiments with Future Linear e^+e^- Colliders, edited by A. Para, H.E. Fisk, Melville 2001, hep-ex/0101005
54. J. Erler, S. Heinemeyer, W. Hollik, G. Weiglein, P.M. Zerwas, Phys. Lett. B **486**, 125 (2000)
55. E. Boos, H.U. Martyn, G. Moortgat-Pick, M. Sachwitz, A. Vologdin, P.M. Zerwas, in preparation
56. M. Carena et al., Nucl. Phys. B **491**, 103 (1997); S.A. Abel, B. Allanach, Phys. Lett. B **415**, 371 (1997)
57. W. Buchmüller, D. Wyler, Phys. Lett. B **521**, 291 (2001)
58. N. Polonsky, A. Pomarol, Phys. Rev. Lett. **73**, 2292 (1994); Phys. Rev. D **51**, 6532 (1995); Y. Kawamura, H. Murayama, M. Yamaguchi, Phys. Rev. D **51**, 1337 (1995)
59. C.F. Kolda, S.P. Martin, Phys. Rev. D **53**, 3871 (1996)
60. G.F. Giudice, R. Rattazzi, Phys. Rept. **322**, 419 (1998)
61. E. Witten, Talk at SUSY02, DESY Hamburg; http://www.desy.de/susy02/
62. S.P. Martin, Phys. Rev. D **55**, 3177 (1997); S. Dimopoulos, G.F. Giudice, A. Pomarol, Phys. Lett. B **389**, 37 (1996)
63. J. Bagger, K. Matchev, D. Pierce, R. Zhang, Phys. Rev. D **55**, 3188 (1997)
64. S. Ambrosanio, G.A. Blair, Eur. Phys. J. C **12**, 287 (2000)
65. B.C. Allanach, D. Grellscheid, F. Quevedo, JHEP **0205**, 048 (2002)
66. C.H. Chen, M. Drees, J.F. Gunion, Phys. Rev. D **55**, 330 (1997); [Erratum ibid. D **60**, 039901 (1999)]
67. L.E. Ibáñez, D. Lüst, G.G. Ross, Phys. Lett. B **272**, 251 (1991); J.P. Derendinger, S. Ferrara, C. Kounnas, F. Zwirner, Nucl. Phys. B **372**, 145 (1992); V.S. Kaplunovsky, Nucl. Phys. B **307**, 145 (1988) [Erratum ibid. B **382**, 436 (1992)]
68. G. Auberson, G. Moultaka, Eur. Phys. J. C **12**, 331 (2000); D. Kazakov, G. Moultaka, Nucl. Phys. B **577**, 121 (2000)
69. L.E. Ibáñez, C. López, Nucl. Phys. B **233**, 511 (1984); L.E. Ibáñez, J. Mas, Nucl. Phys. B **286**, 107 (1987)